Volume 6, Issue 11 – July – December – 2019

ECORFAN

Journal-Bolivia

ISSN-On line 2410-4191

10th ANNIVERSARY ECORFAN Special Edition

ECORFAN Journal-Bolivia, Volume 6, Issue 11, July - December 2019, is a journal edited four- monthly by ECORFAN-Bolivia. Loa 1179, Cd. Sucre. Chuquisaca, Bolivia. WEB: www.ecorfan.org, revista@ecorfan.org. Chief Editor: IGLESIAS-SUAREZ, Fernando. MsC. ISSN-On line: 2410-4191. Responsible for the latest update of this number ECORFAN Computer Unit. ESCAMILLA-BOUCHÁN, Imelda. PhD, LUNA- SOTO, Vladimir. PhD. Loa 1179, Cd. Sucre. Chuquisaca, Bolivia, last updated December 31, 2019.

ECORFAN-Journal Bolivia

Definition of the Journal

Scientific Objectives

Support the international scientific community in its written production Science, Technology and Innovation in the Field of Medicine and Health Sciences, in Subdisciplines Engineering, Chemical, Optical, Resources, Food technology, Anatomy, Nutrition.

ECORFAN-Mexico SC is a Scientific and Technological Company in contribution to the Human Resource training focused on the continuity in the critical analysis of International Research and is attached to CONACYT-RENIECYT number 1702902, its commitment is to disseminate research and contributions of the International Scientific Community, academic institutions, agencies and entities of the public and private sectors and contribute to the linking of researchers who carry out scientific activities, technological developments and training of specialized human resources with governments, companies and social organizations.

Encourage the interlocution of the International Scientific Community with other Study Centers in Mexico and abroad and promote a wide incorporation of academics, specialists and researchers to the publication in Science Structures of Autonomous Universities - State Public Universities - Federal IES - Polytechnic Universities - Technological Universities - Federal Technological Institutes - Normal Schools - Decentralized Technological Institutes - Intercultural Universities - S & T Councils - CONACYT Research Centers.

Scope, Coverage and Audience

ECORFAN -Journal Bolivia is a Journal edited by ECORFAN-Mexico S.C in its Holding with repository in Bolivia, is a scientific publication arbitrated and indexed with semester periods. It supports a wide range of contents that are evaluated by academic peers by the Double-Blind method, around subjects related to the theory and practice of Engineering, Chemical, Optical, Resources, Food technology, Anatomy, Nutrition with diverse approaches and perspectives , That contribute to the diffusion of the development of Science Technology and Innovation that allow the arguments related to the decision making and influence in the formulation of international policies in the Field of Medicine and Health Sciences. The editorial horizon of ECORFAN-Mexico® extends beyond the academy and integrates other segments of research and analysis outside the scope, as long as they meet the requirements of rigorous argumentative and scientific, as well as addressing issues of general and current interest of the International Scientific Society.

Editorial Board

Arbitration Committee

Assignment of Rights

The sending of an Article to ECORFAN -Journal Bolivia emanates the commitment of the author not to submit it simultaneously to the consideration of other series publications for it must complement the Originality Format for its Article.

The authors sign the Authorization Format for their Article to be disseminated by means that ECORFAN-Mexico, S.C. In its Holding Bolivia considers pertinent for disclosure and diffusion of its Article its Rights of Work.

Declaration of Authorship

Indicate the Name of Author and Coauthors at most in the participation of the Article and indicate in extensive the Institutional Affiliation indicating the Department.

Identify the Name of Author and Coauthors at most with the CVU Scholarship Number-PNPC or SNI-CONACYT- Indicating the Researcher Level and their Google Scholar Profile to verify their Citation Level and H index.

Identify the Name of Author and Coauthors at most in the Science and Technology Profiles widely accepted by the International Scientific Community ORC ID - Researcher ID Thomson - arXiv Author ID - PubMed Author ID - Open ID respectively.

Indicate the contact for correspondence to the Author (Mail and Telephone) and indicate the Researcher who contributes as the first Author of the Article.

Plagiarism Detection

All Articles will be tested by plagiarism software PLAGSCAN if a plagiarism level is detected Positive will not be sent to arbitration and will be rescinded of the reception of the Article notifying the Authors responsible, claiming that academic plagiarism is criminalized in the Penal Code.

Arbitration Process

All Articles will be evaluated by academic peers by the Double Blind method, the Arbitration Approval is a requirement for the Editorial Board to make a final decision that will be final in all cases. MARVID® is a derivative brand of ECORFAN® specialized in providing the expert evaluators all of them with Doctorate degree and distinction of International Researchers in the respective Councils of Science and Technology the counterpart of CONACYT for the chapters of America-Europe-Asia-Africa and Oceania. The identification of the authorship should only appear on a first removable page, in order to ensure that the Arbitration process is anonymous and covers the following stages: Identification of the Journal with its author occupation rate - Identification of Authors and Coauthors - Detection of plagiarism PLAGSCAN - Review of Formats of Authorization and Originality-Allocation to the Editorial Board- Allocation of the pair of Expert Arbitrators-Notification of Arbitration - Declaration of observations to the Author-Verification of Article Modified for Editing-Publication.

Instructions for Scientific, Technological and Innovation Publication

Knowledge Area

The works must be unpublished and refer to topics of Engineering, Chemical, Optical, Resources, Food technology, Anatomy, Nutrition and other topics related to Medicine and Health Sciences.

Presentation of the Content

In the first chapter we present, *Influence of anisotropy on the formability of 439 stainless steel*, by SALGADO-LOPEZ, Juan Manuel, OJEDA-ELIZARRARÁS, José Luis, PÉREZ-QUIROZ, José Trinidad and VERGARA-HERNÁNDEZ, Hector Javier, as the following article we present, *Viral and bacterial pneumonia Detection in x-ray images using artificial neural networks*, by GUERRERO-GASCA, Itzel, YAÑEZ-VARGAS, Israel, QUINTANILLA-DOMÍNGUEZ, Joel, LARA-GONZÁLEZ, Luis and GASCA-ORTEGA, Arturo, with ascription in the Universidad Politécnica de Juventino Rosas and the Instituto Tecnológico de Celaya, as the following article we present, *Carbon nanospheres as an electrode material for electroadsorption of Cu (II)*, by KASHINA, Svetlana, BALLEZA, Marco, JACOBO-AZUARA, Araceli, GALINDO-GONZÁLEZ, Rosario, with ascription in the Universidad de Guanajuato, as the following article we present, *Proposed protocol with transcutaneous electrical nerve stimulation for the treatment of non-specific chronic low back pain*, by CORONA-BRISEÑO, Agustin, with ascription in the Universidad del Futbol y Ciencias del Deporte, as the following article we present, *Predictibility and aesthetics in the anterior sector*, by OROZCO-RODRIGUEZ, Rubén, ROSADO-VILA, Graciella, ZAPATA-MAY, Rafael and PINZON-SIERRA, Patricia, with ascription in the Universidad Autonoma de Campeche, as the following article we present, *Sequence of treatment of a labial hemangioma*, ACUÑA-GONZALEZ, Gladys Remigia, MAYA-GARCÍA, Ixchel, ROSADO-VILA, Graciella and ZAPATA-MAY, Rafael, with ascription in the Universidad Autonoma de Campeche.

Content

Article **ECORFAN-Journal Bolivia**
December 2019 Vol.6 No.11 1-8

Influence of anisotropy on the formability of 439 stainless steel

Influencia de la anisotropia en la formabilidad de acero inoxidable 439

SALGADO-LOPEZ, Juan Manuel†*, OJEDA-ELIZARRARÁS, José Luis, PÉREZ-QUIROZ, José Trinidad and VERGARA-HERNÁNDEZ, Hector Javier

Centro de Ingeniería y Desarrollo Industrial, Querétaro, Querétaro, México
Instituto Mexicano del Transporte, Pedro Escobedo, Querétaro, México
Tecnológico Nacional de México/I. T. Morelia, Morelia, 58120, Michoacán, México

ID 1st Author: *Juan Manuel, Salgado-Lopez* / **ORC ID:** 0000-0002-2384-1887, **CVU CONACYT ID:** 94744

ID 1st Coauthor: *José Luis, Ojeda-Elizarrarás* / **ORC ID**: 0000-0001-8412-7778, **CVU CONACYT ID:** 81630

ID 2nd Coauthor: *José Trinidad, Pérez-Quiroz* / **ORC ID:** 0000-0002-7230-9715, **CVU CONACYT ID:** 91805

ID 3rd Coauthor: *Hector Javier, Vergara-Hernández* / **ORC ID:** 0000-0001-6224-1027, **CVU CONACYT ID:** 38689

DOI: 10.35429/EJB.2019.11.6.1.8 Received July 18, 2019; Accepted September 13, 2019

Abstract

This work shows the influence of the normal anisotropy ("r" value) in the deep drawing of AISI 439 ferritic stainless steel sheets. In order to do so, quantitative chemical analysis, metallographic analysis, tensile mechanical properties, and the determination of the "r" value and the "n" value were carried out in two different AISI 439 steel sheets of two different suppliers. In recent years, this ferritic stainless steel has been applied in a deep drawing process of automotive components. In this way, it must be said that one of these ferritic stainless steel sheets cracked due to exhaustion of formability during deep drawing after few steps. On the other hand, the second ferritic stainless steel sheet showed neither cracking nor other type of defects. The results of the tests, which were carried out in this work, probed that the"r" value has a strong influence on the forming behaviour of ferritic steel during deep drawing. This information is very relevant because the AISI 439 standard does not consider the planar anisotropy or the strain hardening coefficient as relevant for designation, but this type of steel is being applied in many forming operations of different components.

Drawability, Ferritic stainless steel, Planar anisotropy

Resumen

Este trabajo muestra la influencia de la anisotropia normal (valor "r") en el proceso embutido de láminas de acero inoxidable ferrítico AISI 439. Para ello se llevó a cabo análisis químico cuantitativo, análisis metalográfico, ensayo mecánico de tensión y determinación de los valores "n" y "r" a muestras de laminas de dos aceros AISI 439 de dos proveedores distintos. Cabe mencionarse que estos materiales eran utilizados en el proceso de troquelado de piezas automotrices y uno de estos aceros presentaban un alto nivel de agrietamiento por agotamiento de formabilidad en los primeros pasos de embutido; mientras que el segundo acero daba un mucho menor nivel defectos y no presentaba grietas después del proceso Los resultados demuestran la importancia de considerar los valores "r" que influyen fuertemente en el comportamiento de este tipo de materiales durante el proceso de embutido. Esta información es aun más relevante si se considera que la especificación para aceros inoxidables ferríticos no consideran estos valores como escenciales para la designación de estos materiales, pero este tipo de aceros es aplicado en el conformado de distintos componentes.

Formabilidad, Acero inoxidable ferrítico, Anisotropia planar

Citation: SALGADO-LOPEZ, Juan Manuel, OJEDA-ELIZARRARÁS, José Luis, PÉREZ-QUIROZ, José Trinidad and VERGARA-HERNÁNDEZ, Hector Javier. Influence of anisotropy on the formability of 439 stainless steel. ECORFAN Journal-Bolivia. 2019. 6-11: 1-8.

* Correspondence to Author (email: msalgado@cidesi.edu.mx)
† Researcher contributing first author.

Introduction

Deep drawing is one of the most important processes in the manufacture of different automotive components and ferritic stainless steel has been used with this process. Therefore, the interest to apply this material in the manufacture of various components has increased [1]. This is especially true regarding the application of this material in processes such as: welding or deep drawing.

However, ferritic stainless steel is usually designated by the chemical composition and mechanical properties of tension, but there is no mention of formability and it is here that basic knowledge on it leads to good results after deep drawing [3]. However, elongation and percentage of area reduction are considered as measures of ductility and thus of formability; but the limit of formality of a material depends not only on such parameters, but also on the deformation ratio, the shear stress ratio and the temperature [4].

In addition, for good results after deep drawing, another very important property of the material to consider is anisotropy, which is also known as the "lakeford parameter" or "r" value. This value can be defined as the resistance to thinning located during the inlay of a material. In other words, this value gives an idea of the homogeneity of the thickness during deformation and this is strongly influenced by the crystallographic texture of the material and, in turn, the texture is influenced by factors such as: type of plastic deformation processes, deformation cycle, heat treatment, winding, etc. [5]. This is especially true when it comes to deep drawing.

In the technical literature, it has been clearly explained that in order to improve the mechanical behavior of a material during deep drawing, some values must be considered in each sheet subject to deep drawing, such as: the strain hardening coefficient ("n" value) and the planar anisotropy ("r" value); but in daily practice such parameters are not considered [6, 7]. This lack of knowledge about the planar anisotropy of ferritic stainless steel sheets leads to production problems such as cracking, ripples, striations, etc., which increases the level of rejection of the production line.

As an example of the above are figures 1 and 2, which show a failed component during the second deep drawing step that was manufactured with AISI 439 ferritic stainless steel.

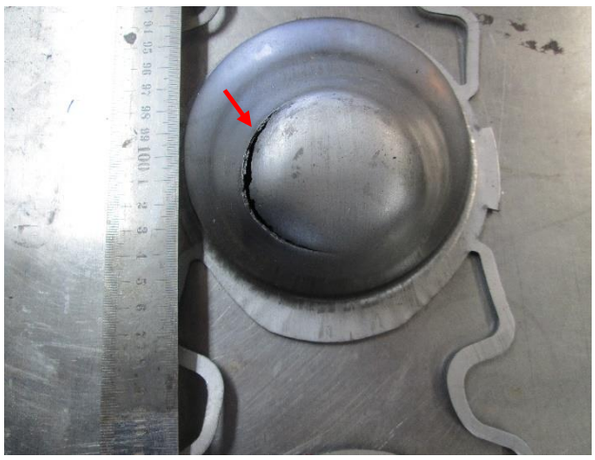

Figure 1 Cracked component in second deep drawing step. It is observed that the crack is located in the inner radius
Source: Prepared by the authors

On the other hand, Figure 3 shows the fracture surface of one of the cracked specimens shown in the previous figures. It can be seen that the fracture is located within the inner radius of the component and evidence of plastic deformation. These figures are evidence of cracks produced by an exhaustion of plasticity during deep drawing.

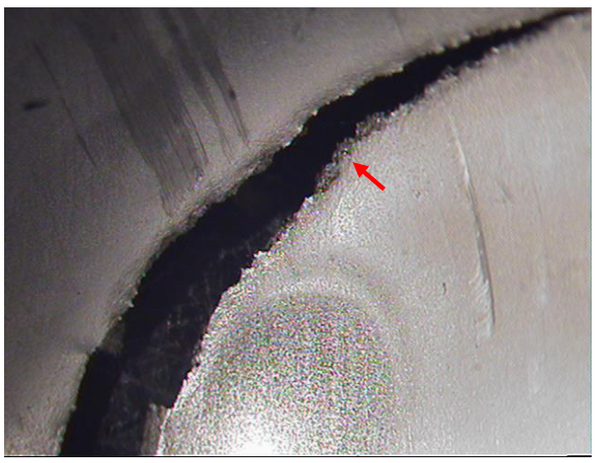

Figure 2 Internal surface of the stamped and cracked component after the second process step. The crack located in the lower radius of the component can be observed
Source: Prepared by the authors

ISSN-On line 2410-4191

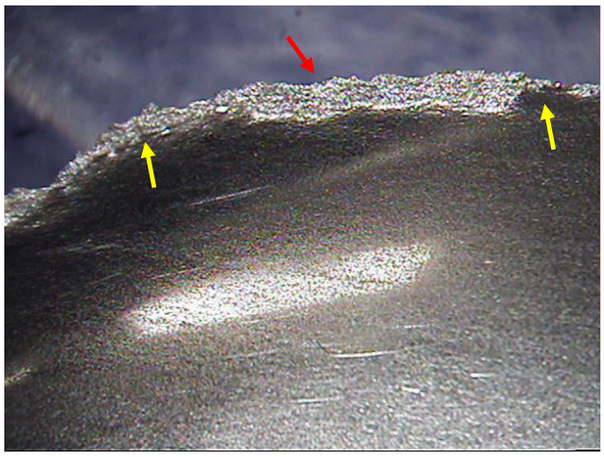

Figure 3 Internal surface of the cracked component after the second deep drawing step. The fracture surface (red arrow) and evidence of plastic deformation (red arrows) can be observed
Source: Prepared by the authors

These failures in the embedded components occurred with sheets of AISI 439 ferritic stainless steel (steel B) which were subject to deep drawing with the same process conditions as sheets of the same material but from a different supplier (steel A), with which this type of problem did not occur. It should be mentioned that with steel A the rejection level was approximately 4%, while steel B gave rejection levels of up to 40% due to cracking in the lower radius of the component. The difference in behavior during deep drawing indicates that, although they were apparently the same material, there were differences between the two which led to different results after the process.

Then, the objective of this paper is to determine the differences between both sheets of AISI 439 ferritic stainless steel that can explain why steel B failed during deep drawing. The results of this work show the importance of the "r" (planar anisotropy) values in ferritic stainless steels that are subjected to deformation and that should be considered when selecting sheets of this material for deep drawing.

In order to achieve the objective of this work, both sheets of ferritic stainless steel were analyzed by means of quantitative chemical analysis, mechanical stress test, metallographic analysis, and determination of the “n” and “r” values of each sheet. Finally, the results of each material were compared to each other.

Methodology

As previously mentioned, two sheets of AISI 439 ferritic stainless steel (steel A and steel B), which apparently had no differences between them but that led to different results after deep drawing, were tested by means of different techniques. It should be noted that the sheet of steel that did not produce cracking after deep drawing was designated as steel A, while the sheet that produced cracking during deep drawing was designated as steel B.

The chemical composition of both ferritic stainless steel sheets was determined by means of the optical emission spectrometry technique using a Espectrolab Lav MB 18B, SPECTRA A220.

For the metallographic analysis of both sheets, samples were cut in the transverse plane to the lamination plane and were prepared to observe the microstructure of ASTM-E03-11. The microstructures were revealed by chemical attack using the Beraha’s reagent [11]. The microstructure was observed using a NIKON EPIPHOT 200 optical microscope with image analyzer.

The mechanical stress test was performed following ASTM-E08-16 [12]. Three specimens of both sheets were tested using an INSTRON model 4482 universal testing machine. It should be mentioned that the longitudinal axes of the cut samples were parallel to the laminate axis of the sheet and elongation was measured using a class B extensometer.

In the same universal tension machine, the “n” values were measured on both sheets (steel A and steel B) according to the ASTM 646-16 standard. This equipment was also used to determine the "r" values according to ASTM 517-00.

The results obtained after each trial were compared and discussed. Evidence and discussion are shown in the following sections.

Results and discussion

The results of the tests that were carried out on both stainless steel sheets of ferritic stainless steel (steel A and steel B) are shown and discussed in this section.

ISSN-On line 2410-4191

First of all, it should be mentioned that a visual inspection was carried out on the specimen that failed during the deep drawing process to identify the characteristics of the fracture. This component was made of B steel. The most important characteristic of the fracture is that it is located in the lower radius and shows evidence of severe plastic deformation.

This evidence indicates that the fracture of steel B was due to a level of deformation which exceeded the deformation that the material could accept. This is called formability depletion and the fact that steel A did not show this crack indicates that this steel can distribute this plastic deformation in a different way than steel B.

On the other hand, the results of the chemical analysis are shown in table 1 for steel A and table 2 for steel B. Comparing the chemical composition of steel A with the chemical composition of steel B shown in the respective tables show that there is no significant difference between both materials and both comply with the specifications of a ferritic stainless steel AISI 439.

In addition, no alloying element was found that could detrimentally influence formability and should be taken into account.

These results showed that the difference in formability is not caused by the effect of the alloying elements of the steels analyzed here. However, it should be mentioned that both steel A and steel B contain titanium.

In fact, the content of this element does not exceed 0.35%, which exceeds the percentage of carbon and it is very difficult for it to be interstitially found.

This fact is important because in the technical literature it is mentioned that this element is a strong builder of carbides and carbonitrides, this fact influences the formability of the materials (in this case they would also have an effect on the “n” and “r” values) [13].

Element	Specification	Result
Carbon	0.07% max.	0.02%
Silicon	1.0% max	0.38%
Phosphorus	0.04% max	0.02%
Manganese	1.0% max.	0.27%
Sulphur	0.030% max.	0.003%
Nickel	0.50% max.	0.18%
Chromium	17.0 -19.0%	17.3%
Aluminum	0.15%	0.02%
Titanium	12xCmin -1.1%	0.34%

Table 1 Results of the quantitative chemical analysis of steel A
Source: Prepared by the authors

Element	Specification	Result
Carbon	0.07% max.	0.02%
Silicon	1.0% max	0.33%
Phosphorus	0.04% max	0.03%
Manganese	1.0% max.	0.27%
Sulphur	0.030% max.	0.003%
Nickel	0.50% max.	0.21%
Chromium	17.0 -19.0%	18.0%
Aluminum	0.15%	0.01%
Titanium	12xCmin -1.1%	0.20%

Table 2 Results of the quantitative chemical analysis of steel B
Source: Prepared by the authors

In the case of the metallographic analysis, this was carried out in the cross section to the fractured surface of the fractured specimen (figure 3), and in the cross sections of steel A and steel B. The microstructure in figure 3 revealed the existence of plastic deformation located in the region near the fracture surface in addition to microcracks originating from non-metallic inclusions. These facts indicate that this material was fractured by localized deformation.

In addition, the micrograph shows that there is a low level of precipitates and there are no corrosion pitting, these facts are consistent with the evidence of the visual inspection and this confirms that the failure occurred due to an overload during the deep drawing process, which caused a ductile fracture due to a deformation located in the lower radius of the embedded specimen. In other words, the fracture was due to depletion of formability.

ISSN-On line 2410-4191

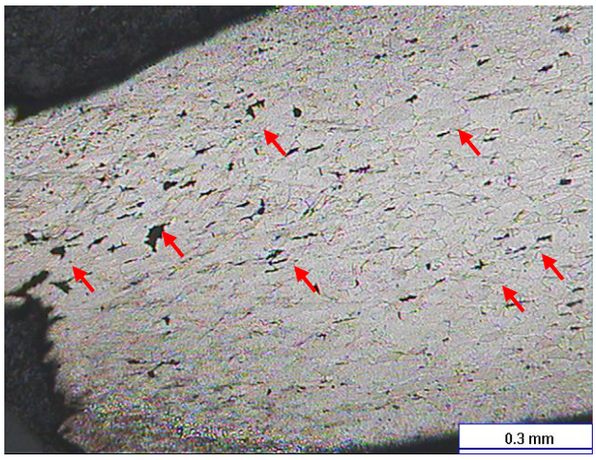

Figure 4 Microstructure at 50X in the region of the fracture surface of steel sheet B. Deformed grains and fracture dimples (red arrows) are observed
Source: Prepared by the authors

Figure 5 shows the microstructure at 100X of steel A and figure 6 shows the microstructure at 100X of steel B. Comparing both microstructures, it is clear that the microstructure of steel B qualitatively has a level of non-metallic inclusions greater than the level of non-metallic inclusions of steel A. This is very important because in the technical literature the great influence of non-metallic inclusions on mechanical properties of the material has been reported, such as: reduction of stress test area, and especially resistance to fatigue. It is important to mention that the type of non-metallic inclusions and the distribution of these have an effect on the mechanical properties, especially regarding oxides, silicates, etc. [14].

Figure 5 Microstructure at 100X of steel A. Recrystallized grains are observed
Source: Prepared by the authors

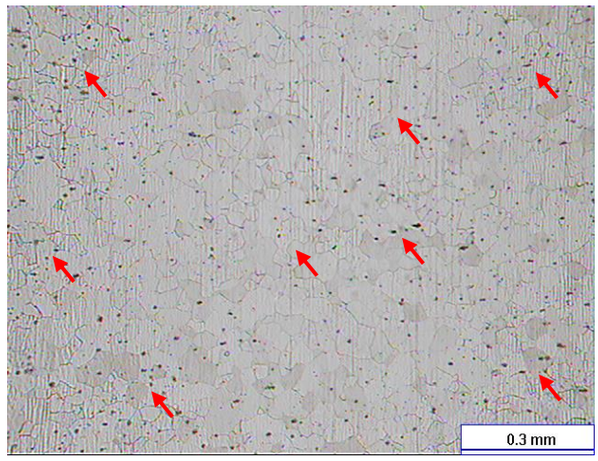

Figure 6 Microstructure at 100X of steel B. Recrystallized grains and non-metallic inclusions (red arrows) are observed
Source: Prepared by the authors

The fracture analysis was performed using a JEOL brand scanning electron microscope (SEM). Figures 7 and 8 show the fracture surface of the fractured specimen in the second deep drawing step. The image shows the crack fracture pattern, which consists of tearing fracture dimples and non-metallic inclusions. These evidences confirmed that the fracture of this embedded component was due to ductile overload that led to a depletion of formability. These evidences agree with the metallographic analysis and visual inspection.

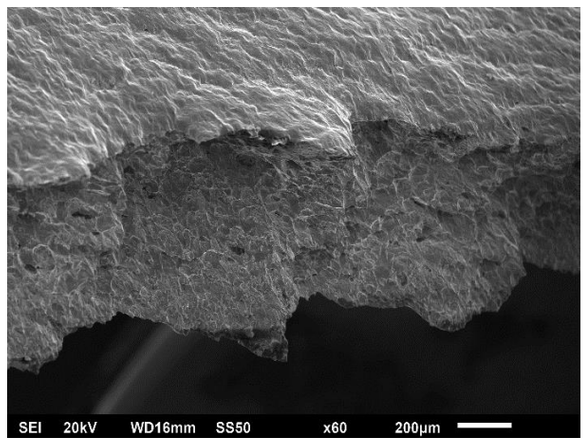

Figure 7 Fractography of the cracked specimen
Source: Prepared by the authors

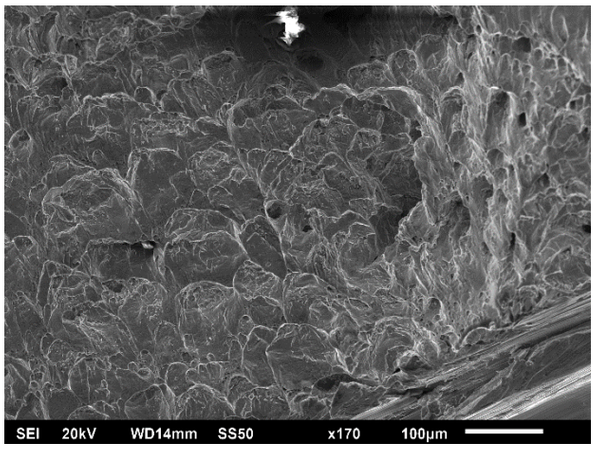

Figure 8 Fracture pattern of the crack shown in the previous figure. Fracture dimples are observed
Source: Prepared by the authors

In the same way, the SEM inspection which was carried out on the outer surface of the cracked specimen in the second deep drawing step showed microcracks and amicroscopic plastic deformation. This is shown in Figure 9 and these evidences indicated that the microcracks were generated by ductile deformation. Again, these results agree with the cause of ductility depletion.

At this point it was necessary to determine the mechanical properties of both stainless steel sheets (steel A and steel B) in order to find some difference between them. The results of the mechanical stress tests performed are shown in table 3 and table 4.

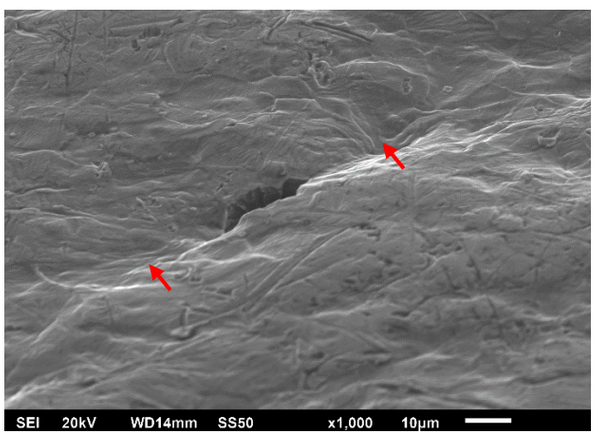

Figure 9 SEM image of the outer surface of the specimen cracked in deep drawing. Microcracks and microscopic plastic deformation (plastic deformation) are observed
Source: Prepared by the authors

The results of mechanical stress tests showed that there was no substantial difference between steel A and steel B in terms of yielding or elongation.

However, a difference of 27.9 MPa (or 40.74 kSI) was found in the ultimate tensile strength (UTS) between steel A and steel B.

This difference can be explained by the higher level of nonmetallic inclusions of steel B with respect to steel A.

In the same way, normal anisotropy (“r” value) and strain hardening coefficient (“n” value) were determined and the results clearly show a significant difference in the planar anisotropy value or “r” values between steel A and steel B.

Tables 5 and 6 show the results of the measurements of the “n” and “r” values of both sheets.

This is so, considering that a variation in the value "r" of 0.5 is considerable and this explains the difference in behavior during the plastic deformation between the two steels.

Results steel A	MPa	kSI
UTS	464.81	674.14
Yielding effort	294.4	426.96
Elongation (%)	34.16	34.16

Table 3 Results of the measurement of the mechanical properties to tension of steel A
Source: Prepared by the authors

Results steel B	MPa	kSI
UTS	436.85	633.4
Yielding effort	279.52	405.4
Elongation (%)	35.12	35.12

Table 4 Results of the measurement of the mechanical properties to tension of steel B
Source: Prepared by the authors

Steel A

Results	Steel A	Average
“r” value at 0 °	1.494	1.565
“r” value at 45°	1.369	
“r” value at 90°	2.031	
“n” value at 0°	0.230	0.223
“n” value at 45°	0.219	
“n” value at 90°	0.217	

Table 5 Results of the measurement of the “n” and “r” values of steel A
Source: Prepared by the authors

Steel B

Results	Steel B	Average
“r” value at 0 °	0.90	1.03
“r” value at 45°	0.83	
“r” value at 90°	1.55	
“n” value at 0°	0.223	0.220
“n” value at 45°	0.226	
“n” value at 90°	0.223	

Table 6 Results of the measurement of the "n" and "r" values of steel B
Source: Prepared by the authors

In the technical literature it has been reported that a planar anisotropy value greater than 1 is recommended to obtain good results during deep drawing operations [5]. In the same way, it has been proven that the value "r" is strongly influenced by the texture of the steel sheet and, in turn, this is modified by the rolling process and the heat treatment of annealing both in winding and after cold rolling. This means that differences in the type of rolling, number of rolling steps, winding temperatures, annealing temperatures, treatment time, give rise to differences in the "r" and "n" values (although in this case the values of "n" were very similar) due to differences in the intensity of the components of the crystallographic texture and with it in the results during deep drawing. This difference will be reflected in the mechanical properties by the formation of defects such as cracking in a ductile manner (as is the case presented here), the formation of wrinkles, or stretch marks [17-20].

This evidence is connected to the results of many previous investigations and this allows us to say that the difference in behavior during deep drawing can be attributed to differences in the processing of sheet A with respect to sheet B. However, it should be mentioned that the authors did not have access to information from suppliers of material A or material B, as it was considered restricted as industrial secret.

Appendage

All tables and figures were obtained by the authors in the CIDESI metallography and failure analysis laboratory in Queretaro, Mexico.

In addition, the authors wish to thank CIDESI for the support provided during this work.

Conclusions

The previously discussed facts lead to the following conclusions:

1. The results indicated that the difference in behavior during plastic deformation and in its results between both sheets of ferritic stainless steel (steel A and steel B) can be attributed to the difference between planar anisotropy values ("r" values).

2. The difference in normal anisotropy ("r" value) can be attributed to a difference in the processing parameters (time, temperature, strain ratio, etc.).

3. Planar anisotropy should be taken into account when ferritic stainless steel sheets are selected for deep drawing.

4. The results indicated that "r" values greater than 1.5 lead to good results during deep drawing.

5. Non-metallic inclusions play a role during deformation or fracture during deformation and fracture of ferritic stainless steel sheets.

References

[1] Groveer M. P. Fundamentals of modern manufacturing. United States of America: John Wiley & Sons, Inc. 2010.700P.

[2] International Stainless Steel Forum (ISSF). Propiedades, Ventajas, Aplicaciones. 1140 Brussels • Belgium: ISSF. April 2007.

[3] Xiang-mi, Y. O. U., Zhou-hua, J. I. A. N. G., & Hua-bing, L. I. (2007). Ultra-Pure Ferritic Stainless Steels—Grade, Refining Operation, and Application. *Journal of Iron and Steel Research, International*, *14*(4), 24-30.

[4] ASTM subcomitte A240. Specification for Heat-Resisting Chromium and Chromium-Nickel Stainless Steel plate, Sheet and Strip for Pressure Vessels.

[5] Emmens, W. C. (2011). Formability: A review of parameters and processes that control, limit or enhance the formability of sheet metal. Springer Science & Business Media.

ISSN-On line 2410-4191

[6] Banabic, D., Bünge, H. J., Pöhlandt, K., & Tekkaya, A. E. (2000). Formability of Metallic Materials (Plastic Anisotropy, Formability Testing and Forming Limits), Editor: Banabic D.

[7] Hutchinson, W. B. (1984). Development and control of annealing textures in low-carbon steels. International metals reviews, 29(1), 25-42.

[8] Levy, B. S., & Van Tyne, C. J. (2008). Failure during sheared edge stretching. *Journal of materials engineering and performance*, *17*(6), 842-848.

[9] Huh, M. Y., & Engler, O. (2001). Effect of intermediate annealing on texture, formability and ridging of 17% Cr ferritic stainless steel sheet. Materials Science and Engineering: A, 308(1-2), 74-87.

[10] ASTM International. ASTM designation: E112 – 13, Standard Test Methods for Determining Average Grain Size1. 3p.

[11] ASTM subcomitte E04.01, ASTM-E03-11: Standard Guide for Preparation of Metallographic Specimens, p.12, 2011.

[12] ASTM Subcomitte E028.04, ASTM-E8/E8M − 16a: Standard Test Methods for Tension Testing of Metallic Materials, p.29, 2016.

[13] ASTM subcomitte E517-00, ASTM – E517-00. Standard Test Method for Plastic Strain Ratio *r* for Sheet Metal.

[14] ASTM Subcomitte E646-16, ASTM – E646-16. Standard Test Method for Tensile Strain-Hardening Exponents (n -Values) of Metallic Sheet Materials.

[15] Ishimaru, E., Takahashi, A., & Ono, N. (2010). Effect of Material Properties and Forming Conditions on Formability of High-Purity Ferritic Stainless Steel. Nippon Steel Technical Report, (99), 26-32.

[16] Thornton, P. A. (1971). The influence of nonmetallic inclusions on the mechanical properties of steel: A review. Journal of Materials Science, 6(4), 347-356.

[17] Dieter, G. E., Kuhn, H. A., & Semiatin, S. L. (Eds.). (2003). *Handbook of workability and process design*. ASM international.

[18] Zhang, C., Liu, Z., & Wang, G. (2011). Effects of hot rolled shear bands on formability and surface ridging of an ultra purified 21% Cr ferritic stainless steel. *Journal of Materials Processing Technology*, *211*(6), 1051-1059.

[19] Wei, D. U., Jiang, L. Z., Sun, Q. S., Liu, Z. Y., & Zhang, X. (2010). Microstructure, texture, and formability of Nb+ Ti stabilized high purity ferritic stainless steel. *Journal of Iron and Steel Research, International*, *17*(6), 47-52.

[20] Gao, F., Liu, Z., Liu, H., & Wang, G. (2013). Texture evolution and formability under different hot rolling conditions in ultra purified 17% Cr ferritic stainless steels. *Materials Characterization*, *75*, 93-100.

ISSN-On line 2410-4191

Article **ECORFAN-Journal Bolivia**
December 2019 Vol.6 No.11 9-16

Viral and bacterial pneumonia Detection in x-ray images using artificial neural networks

Detección de Neumonía viral y bacteriana en imágenes de rayos x utilizando redes neuronales artificiales

GUERRERO-GASCA, Itzel†*, YAÑEZ-VARGAS, Israel, QUINTANILLA-DOMÍNGUEZ, Joel, LARA-GONZÁLEZ, Luis and GASCA-ORTEGA, Arturo

Universidad Politécnica de Juventino Rosas. Departamento de Ingeniería Telemática, Hidalgo 102, Comunidad de Valencia, Santa Cruz de Juventino Rosas, Gto.
Tecnológico Nacional de México-Instituto Tecnológico de Celaya. Antonio García Cubas Pte #600 esq. Av. Tecnológico. Celaya, Gto. México.

ID 1st Author: *Itzel Guadalupe, Guerrero-Gasca* / **ORC ID:** 0000-0002-7738-5151

ID 1st Coauthor: *Juan Israel, Yañez-Vargas* / **ORC ID:** 0000-0001-5749-8442, **CVU CONACYT ID:** 295711

ID 2nd Coauthor: *Joel, Quintanilla-Domínguez* / **ORC ID:** 0000-0003-2442-2032

ID 3rd Coauthor: *Luis Rey, Lara-González*

ID 4th Coauthor: *Arturo, Gasca-Ortega* / **ORC ID:** 0000-0003-2499-2449

DOI: 10.35429/EJB.2019.11.6.9.16 Received: July 16, 2019; Accepted: September 20, 2019

Abstract

This paper presents the experiments and results on the viral and bacterial pneumonia identification, which were obtained by means of image processing techniques and artificial neural networks. The objective of this research is to reduce the patient's waiting time to obtain the result of the x-rays diagnosis of a pulmonary disease of pneumonia. At the time of this writing, pneumonia is considered the most common cause of infant mortality in the world, responsible for 15% of all deaths in children under 5 years. To obtain the classifier model we start from the detection in the pulmonary region through digital image processing and obtaining the characteristics in the segmented images, discriminating against those that provide a diagnosis through Gray Level Co-occurrence Matrix (GLCM). Finally, those features are used as the description in the classification of images such as: healthy, viral pneumonia and bacterial pneumonia. We use a total of eight features: autocorrelation, contrast, cluster prominence, variance cluster shade, sum of entropy, difference of entropy and number of pixels. These characteristics were used to model and train an artificial neural network Backpropagation, obtaining results that are presented in their confusion matrix along with the accuracy percentage obtained.

X-Ray, Pneumonia, Backpropagation

Resumen

En el presente artículo se presentan los experimentos y resultados obtenidos en la identificación de neumonía viral y bacteriana mediante técnicas de procesamiento de imágenes y redes neuronales artificiales. El objetivo de esta investigación es reducir el tiempo de espera del paciente para obtener el resultado del diagnóstico de rayos X en la enfermedad pulmonar de neumonía. En la actualidad la neumonía se considera la causa más común de mortalidad infantil en el mundo, responsable del 15% de todas las defunciones en menores de 5 años. Para obtener el modelo clasificador partimos de la detección en la región pulmonar a través de procesamiento digital de imágenes y la obtención de las características en las imágenes segmentadas, discriminando aquellos que nos proporcionen un diagnóstico a través de Gray Level Co-occurrence Matrix (GLCM). Finalmente, dichas características son utilizadas como la descripción en la clasificación de imágenes como son: predictores en la clasificación y diagnóstico de las imágenes: Sin Neumonía (sano), Neumonía Viral y Neumonía Bacteriana. Usamos un total de ocho características: autocorrelación, contraste, cluster prominence, varianza, cluster shade, suma de entropía, diferencia de entropía y numero de pixeles. Dichas características fueron utilizadas para modelar y entrenar una red neuronal artificial, obteniendo los resultados que se ven expresados en su matriz de confusión con el porcentaje de clasificación obtenido.

X-Ray, Neumonía, Backpropagation

Citation: GUERRERO-GASCA, Itzel, YAÑEZ-VARGAS, Israel, QUINTANILLA-DOMÍNGUEZ, Joel, LARA-GONZÁLEZ, Luis and GASCA-ORTEGA, Arturo. Viral and bacterial pneumonia Detection in x-ray images using artificial neural networks. ECORFAN Journal-Bolivia. 2019. 6-11: 9-16.

* Correspondence to Author (email: 315030042@upjr.edu.mx)
† Researcher contributing as first author

1. Introduction

The National Heart, Lung and Blood Institute (Institute, 2018) defines pneumonia as a bacterial, viral or fungal infection of one or both sides of the lungs that causes the alveoli to be filled with microorganisms, inflammatory cells or fluids, which cause an abnormal dysfunction of the lungs. Symptoms may worsen in children under five years of age, which is why it is considered the main cause of infant mortality in the world, responsible for 15% of all deaths in children under 5 years. The World Report on Pneumonia of the World Health Organization (Health, 2016) addressed that the prevention and diagnosis of pneumonia is of fundamental importance for the reduction of infant mortality. Chest X-ray remains the most important diagnostic method that is easily accessible, fast, economical and effective. However, to discriminate between bacterial pneumonia and viral pneumonia, it is difficult to find the diagnosis based on X-rays, which is why the specialist requires more specific tests such as laboratory tests, which implies a greater expenditure of both time and money. Nevertheless, chest images contain abundant noise caused by the thoracic cage, the clavicle, the complex lung structure, the position of the arms at the time of obtaining the radiograph and the subtle texture on the chest radiograph. Segmentation of the region of interest, in this case the lung area, will be a preliminary step to detect the type of pneumonia that the patient presents. The purpose of this document is to establish a tool for analysis of pneumonia infections using algorithms for processing infected and normal X-ray images from the segmentation and extraction of characteristics with the GLCM method; its study is linked to certain works and applications that will be mentioned throughout the document.

2. Related Works

The growth in the field of digital image processing in medical images has given a new dimension to the detection and diagnosis of diseases. Standard chest radiography has been identified as the most complex imaging tool. However, there are different techniques for both segmentation, as well as the classification of lung diseases, which propose to detect lung regions in chest X-ray images contributing to an important component for diagnosis (Sema Candemir, 2014).

Other techniques apply two steps ranging from image enhancement and image filter, where the intensity and contrast of the X-ray image is adjusted to adapt the subsequent stages of processing, using histogram equalization (SR Abhishek Sharma, 2015). Other studies propose a computer-assisted system to identify bacterial and viral pneumonia, classifying it from an SVM support vector machine (Xianghong Gu, 2017).

For this study the main contributions are:

- Obtaining lung segmentation to develop a diagnosis and detection of pneumonia based on an image segmentation algorithm.
- Extraction of mathematical characteristics in the segmented image from the GLCM method.
- Training the neural network and compare models with different layers and neurons for image classification.

The acquired image is segmented from the combination of certain image processing algorithms that will be mentioned in the next section, followed by the calculation and extraction of features. A trained classifier will classify the chest X-ray image samples as healthy or not healthy. The work will culminate in making a final classification with not healthy images where the diagnosis of viral pneumonia and bacterial pneumonia occurs.

3. Data set

The standard digital image database created, *Chest X-Ray Images* (Features, 2018), is used for training and testing purposes; it is organized in 3 folders (train, test, val) and contains subfolders for each image category (pneumonia/normal) with a total of 84,495 X-ray images (JPEG) and 2 categories (pneumonia/normal). These chest X-ray images were selected from pediatric patients of approximately one and five years of the Guangzhou Women's and Children's Medical Center. All chest radiographs were performed as part of the usual clinical care of the patients. For the purpose of this work they were resized to 512x512 pixels and reduced to 8-bit gray scale levels. The database can be useful for various educational and research purposes, along with other demonstrations.

ISSN-On line 2410-4191

4. Feature Extraction

Feature extraction is the process of reducing the data size of each image by obtaining the necessary information from the segmented image. From the extracted characteristics it is possible to depend on the segmentation method and the extracted characteristics. In this work, the characteristic matrix is obtained using Gray Level Co-occurrence Matrix (GLCM) (Shijin Kumar P.S, Extraction of Texture Features using GLCM and Shape Features using Connected Regions, 2017). Images with Viral Pneumonia, Bacterial Pneumonia and Healthy have different characteristics. This variation in the values obtained by characteristics is useful for the classification of X-ray images. The values of the characteristics obtained will be delivered in a test and training classifier. From GLCM, it extracts the statistical characteristics of texture, where we will take 8 texture parameters such as: autocorrelation, contrast, cluster prominence, cluster shade, sum of entropy, difference of entropy, variance and number of pixels.

Texture parameters	Formula	Description
Autocorrelation	$\sum_{K=0}^{N-1-n} I(m,n+k)^2 I(m,k)^2$	Comparison of each pair of pixels to find the probability that their intensity is the same given a specific direction and distance.
Cluster Prominence	$\sum\sum(i+j-\mu-\mu)^3 X\ P(i,j)$	Asymmetry measurement which indicates whether the prominence value of the cluster is high, the image is less symmetrical and when the prominence value of the group is low, there is a peak in the GLCM matrix around the mean values.
Cluster Shade	$\sum\sum(i+j-\mu-\mu)^4 X\ P(i,j)$	Measurement of matrix asymmetry and is believed to measure the perceptual concepts of uniformity. A new I + j image is created, with a range of integer intensities of 0 and 2 (N g-I).
Variance	$\sum_{i=1}^{N}\sum_{j=1}^{N}(i-\mu)^2 p(i,j)$	Measures the dispersion (with respect to the average) of the gray level distribution.
Entropy sum	$-\sum_{i=1}^{N}\sum_{j=1}^{N} px+y(i)\log[Px+y(i)]$	Measures the disorder related to the distribution of the gray levels of the image.
Entropy difference	$-\sum_{i=1}^{N}\sum_{j=1}^{N} px-y(i)\log[Px-y(i)]$	Measures the disorder related to the distribution of the gray level difference of the image.

Table 1 GLCM texture parameter formulas

Where *p (i, j)* is the probability of occurrence of the element *(i, j)* in the GLCM, L is the quantization level, and the vector $P_{x+y}(k) = \sum_{i=1}^{L}\sum_{j=1}^{L} P(i,j)$ for *k = 2, 3,..., 2L.*

For more information consult (P. Mohanaiah, 2013).

5. Methodology

This section details the proposed techniques for the detection of pneumonia which includes three stages: pulmonary segmentation, feature extraction and classification. The representation of the flow chart of our system is presented in Figure 1 and the mentioned steps are explained in detail.

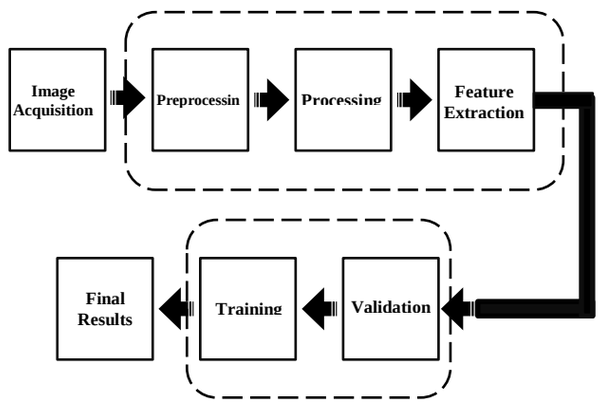

Figure 1 General Diagram

A. Pulmonary Segmentation

From the general diagram, we start in two blocks for the implementation and development of the project. The first stage corresponds to the methodology of digital image processing, as seen in Figure 2.

ISSN-On line 2410-4191

The image is acquired, a pre-processing and processing are carried out and at the end we obtain the segmented image, each of the mentioned processes will be described later.

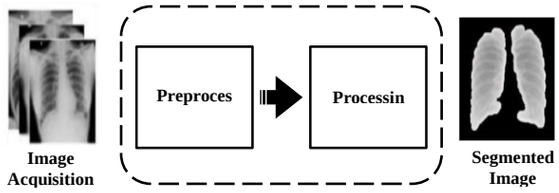

Figure 2 Diagram for image processing

The Matlab software was used to develop the algorithm. The contrast improvement method (The MathWorks, 2019) is used to optimize the performance of lung segmentation. We use a normalization method, which creates a certain independence of the image's properties, later a histogram equalization algorithm is used (Histeq, 2019), opting for Enhace contrast using histogram equalization (Histeq), where the lung area stands out best. The Otsu method (Otsu, 2019), unlike the pixel intensities of each region, separates the foreground image objects and the background image objects, illuminating the specific area. The input is a grayscale or color image and results in a binary image (in black and white) that indicates the segmented part. The preparation of the mask includes morphological measures, as well as the method of erosion, inversion, edge cleaning, removal of small objects and dilation. Figure 3 shows the methodological proposal for this section.

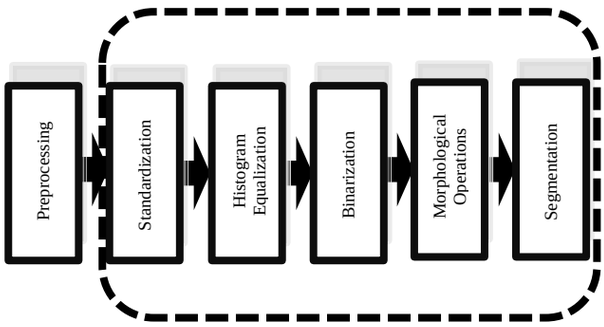

Figure 3 Methodological proposal

The segmented lung image is obtained by multiplying the mask by the original image, as shown in Figure 4, then delivered to the feature extraction stage.

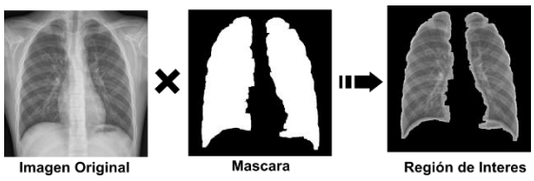

Figure 4 Lung segmentation

B. Feature Extraction using GLCM

The second stage corresponds to the extraction of the characteristics in the segmented image, in the third stage a training and validation is carried out from various tests to finally contribute to the expected result, as shown in Figure 5.

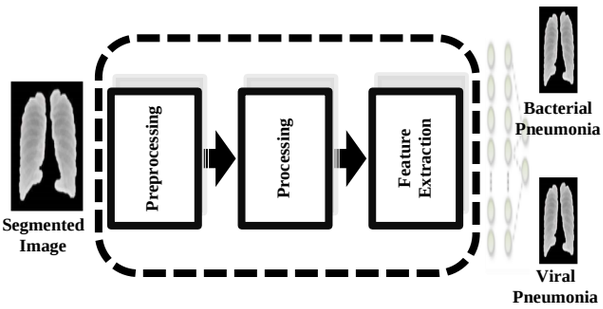

Figure 5 Diagram of the method of image classification

Gray Level Co-occurrence Matrix (GLCM) is calculated by counting the number of times that adjacent pixels have the same orientation (Shijin Kumar P.S, Extraction of Texture Features using GLCM and Shape Features using Connected Regions, 2017).

There are a total of 20 GLCM functions for each segmented region. The average value is calculated from eight basic features: autocorrelation, contrast, prominence cluster, cluster shade, entropy sum, entropy difference, variance and number of pixels. The data that gave us the best results were those shown in Table 2, where the result with the greatest difference was the one considered.

Features	Healthy/Not Healthy
Autocorrelation	5541.45
Contrast	4267.8
Cluster Prominence	629858000
Cluster Shade	1104369
Variance	91345.1
Entropy sum	23203.5
Entropy difference	4267.8

Table 2 Data used for feature extraction

With the features that make up elements for the discrimination of results, an 8x30 training matrix is created for general training and 8x15 for general validation (Healthy/Not healthy). And 8x20 for specific training and 8x10 for specific validation (viral pneumonia/bacterial pneumonia). Figure 6 shows the creation of the input matrix.

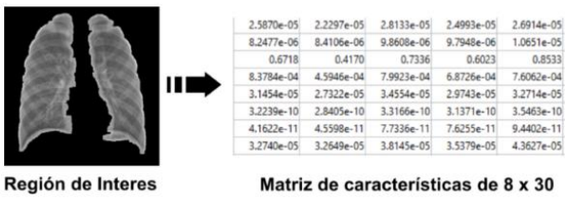

Figure 6 Steps to create the characteristics matrix

C. Classification with Backpropagation

The neural network has two operation techniques: training and validation (Rahmati, 2014). The training set consists of 30 images: 10 healthy images and 20 not healthy images, giving a 30x8 matrix for training the neural network. The validation set consists of a total of 15 images: 5 healthy images and 10 not healthy images. All data corresponds to the information that flows through the network in the learning phase. The learning algorithm used is Backpropagation, which was already mentioned above as a supervised learning algorithm. This learning algorithm applies to multilayer advance networks that consist of processing elements (neurons) with continuous differentiable activation functions (tan-sigmoid and log-sigmoid). Matlab offers specialized libraries to work with neural networks through its tools and functions for managing large data sets. Figure 7 shows the distribution of the classification.

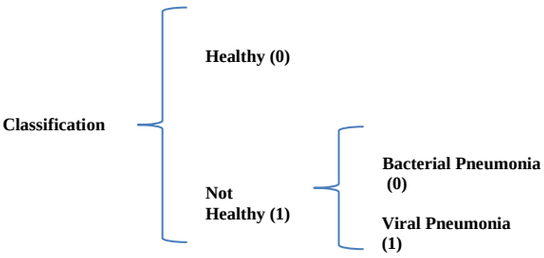

Figure 7 General diagram of the distribution for classification

The trained set of the Healthy images are labeled as class 0 and the Not-Healthy images are labeled as class 1.

In turn, the not healthy images are divided into the subclasses Viral Pneumonia class (1) and Bacterial Pneumonia class (0).

6. Results

The purpose of the segmentation stage was to isolate the anatomical regions of interest from the medical image; for this purpose contrast enhancement techniques and morphological methods were used to reduce noise such as shadows on clavicles and spine. The learning phase was carried out following the Backpropagation technique using a subset of the Chest X-Ray Images (84,495 images). The subset of data (45 images in total) was divided into 30 (66.7%) training elements and 15 (33.3%) validation elements. All images were resized to a size of 512x512 pixels.

The final result for the segmentation part is seen in Figure 8.

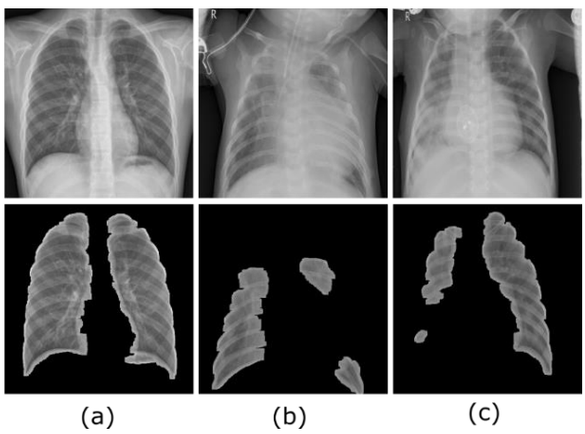

Figure 8 Segmented image of a healthy lung (a), lung with viral pneumonia (b) and lung with bacterial pneumonia (c)

Not all images of Chest X-Ray Images worked and gave us the ideal result. 75 samples were contemplated by selecting 45 which did not lose fundamental information when processed. In the failed cases we lost a part of the lung or the entire pulmonary region, or the opposite happened, where more information was leaked, for example clavicles, shoulders etc. As shown in Figure 9.

ISSN-On line 2410-4191

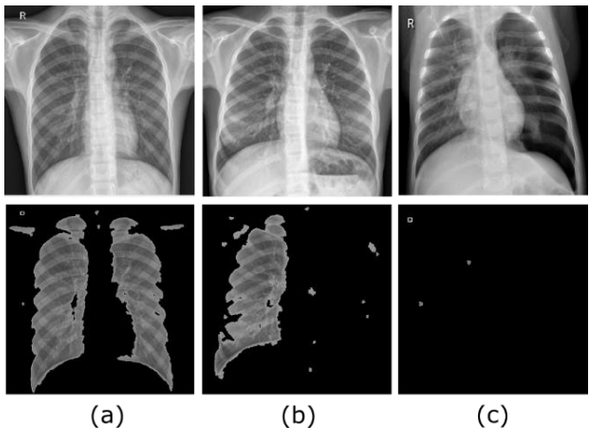

Figure 9 Image of lungs and clavicles (a), image with a single segmented lung (b) image with no segmentation

The RNA architecture based on the Backpropagation training technique is divided into two tests: the first to classify between healthy and not healthy lungs, the second is to classify not healthy lungs in bacterial pneumonia and viral pneumonia.

A. Classification Healthy/Not healthy

Before starting the training of the neural network for the first classification, our parameters were established as: 10,000 times, performance objective of 0.01 and a learning rate of 0.1. The architecture consisted of 8 inputs, 1 output layer and a varied number of hidden layers and the neurons that made them up. Table 3 shows some of the best models and results obtained in the training and validation stages, taking into account the number of layers and neurons, as well as their classification, both correct and incorrect.

Tests No.	Layers and Values	Correct Classification	Incorrect Classification
1	[16,32]	66.66%	33.33%
2	[16,32,64]	80%	20%
3	[20,32,64]	80%	20%
4	**[16,32,64]**	**86.66%**	**13.33%**
5	[5,20,25]	80%	20%
6	[5,15,20]	80%	20%
7	**[5,10,15]**	**86.66%**	**13.33%**

Table 3 Healthy / Not healthy RNA Test

Model 4 and 7 of Table 3 of RNA designed in Matlab, gave us the best classification result for HEALTHY/NOT HEALTHY image recognition. The first model is composed of 8 inputs, three hidden layers with [**16 32 64**] neurons and one output layer.

The second best model made use of fewer neurons in its hidden layer, which decreases the time in the processing and resources of the PC, is made up of 8 inputs, three hidden layers with [**5 10 15**] neurons and one output; so far it is taken as the best model, since it obtains good results using fewer resources.

The confusion matrix of each of the models can be seen in Figure 10, where we will only show the prediction of the Second model (test number 7), which obtains 3 True Positives (TP) and 2 False Negative (FN), for the other test we obtained 0 False Positive (FP) and 10 True Negative (TN).

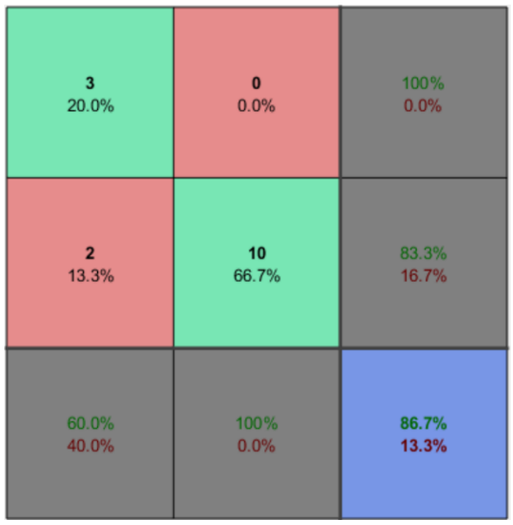

Figure 10 Confusion matrix of the general classification

B. Classification Bacterial Pneumonia / Viral Pneumonia

Table 4 shows some of the tests performed for the classification of not healthy images (Bacterial Pneumonia/Viral Pneumonia), with parameters of 10,000 times, learning rate of 0.1 and a performance objective of 0.01 for each of the tests, these being the same parameters that were stipulated in the beginning.

Tests No.	Layers and Values	Correct Classification	Incorrect Classification
1	[16,32]	50 %	50 %
2	**[16,32,64]**	**80%**	**20%**
3	[20,32,64]	70%	30%
4	[20,35,64]	70%	30%
5	**[16.32,64]**	**90%**	**10%**
6	[10,20,25]	60%	40%
7	[5,15,20]	70%	30%
8	[5,10,20]	70%	30%

Table 4 Bacterial / Viral Pneumonia RNA Test

ISSN-On line 2410-4191

Of the tests carried out, test 2 and 5 of Table 4 of RNA designed in Matlab gave us a better classification result for image recognition Bacterial Pneumonia/Viral Pneumonia. The tests contain 8 inputs, three hidden layers with [16 32 64] neurons and one output layer.

Figure 11 shows the structure of our RNA

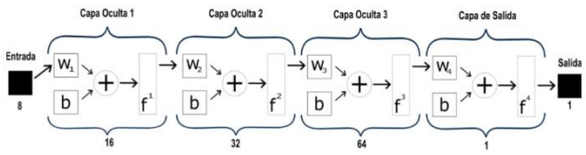

Figure 11 RNA architecture for the NOT HEALTHY classification

We will only expose the model that obtained the best performance (test 5): its confusion matrix (Figure 13) shows results in positive predictions of 5 TP and 0 FN, for negative predictions 1 FP and 4 TN, obtaining only a bad prediction in the Classification of Viral Pneumonia, which discriminated it as Bacterial Pneumonia, this classification had a percentage of 90% of success.

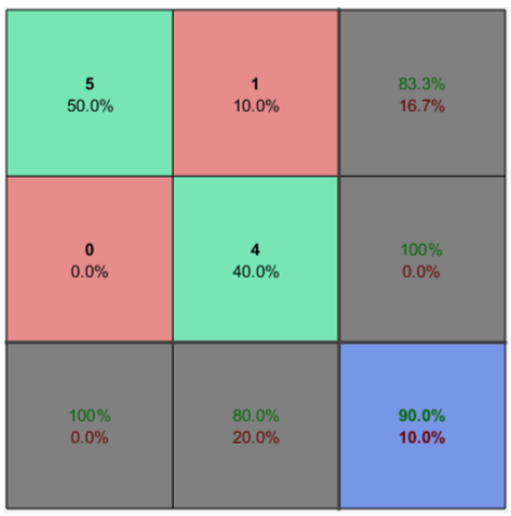

Figure 12 Confusion matrix of the specific classification

A supervised training was carried out where the known set of input-output data was used to adjust the weights of our network. As in the previous model, the performance objective was set at 0.01 for greater accuracy and a total number of 10,000 times. Under these parameters, it was avoided to reach overtraining, that is, a state in which the network adapts so perfectly to the training set that it is unable to generalize and correctly classify new images.

Conclusions

In this paper, the implementation of a diagnosis system of viral and bacterial pneumonia through X-ray images, using digital image processing was proposed, some of our images did not give the expected results, so the decision was made to manually select those images that allowed us to filter the pulmonary region of interest. However, it is proposed an improvement in the image processing algorithm that is deeper than generalize any image that enters and can process it in the broadest way.

For texture extraction, texture analysis using the Gray-Level Cooccurrence Matrix (GLCM) was used, which, through statistical methods, examines the texture that considers the spatial relationship of the pixels in the co-occurrence matrix of the level of gray. Data were chosen that pronounced a considerable difference between the HEALTHY and NOT HEALTHY data. It was the best solution to achieve significant changes in our training network compared to the results obtained in validation.

The methodological tests carried out at work have shown that, through the results expressed in the suggested articles, we achieved good results; the tests corresponding to processing have details for the Chest X-Ray Images file. Therefore the search for the improvement of the algorithm is proposed, as well as cross-validation and use of deep learning with deep convolutions neural networks to compare their results with the proposed method.

The model will help to provide solutions in the area of Health Sciences and patients with a pneumonia pattern with their respective radiography. The type of pneumonia they are presenting will be detected at the time and will also save time in diagnosis as well and it will imply an additional expense. Regarding the specialist, now they will have a tool that will help them, when giving such diagnoses.

References

Features, G. t. (2018). GLCM textures features. Retrieved from https://es.mathworks.com/matlabcentral/fileexchange/22187-glcm-texturefeatures

ISSN-On line 2410-4191

Histeq, M. (2019). Histeq. Retrieved from https://es.mathworks.com/help/images/ref/histeq.html

Institute, L. N. (2018). Pneumonía . Retrieved from https://www.nhlbi.nih.gov/healthtopics/pneumonia

J. K. A. R. M. V. Rahmati, M. H. (2014). "Back propagation artificial neural network structure error reduction by defined factor of capacity and algorithm reinforcement method. International Journal of Soft Computing and Engineering (IJSCE).

Otsu, M. (2019). Graythresh. Retrieved from https://es.mathworks.com/help/images/ref/graythresh.html

P. Mohanaiah, P. S. (2013). Image Texture Feature Extraction Using GLCM Approach. International Journal of Scientific and Research Publications.

Reinhart, C., Reinhart, V., & Rogoff, K. (2012, April). Debt Overhangs: Past and Present. National Bureau of Economic Research Working Paper(18015), 1-29.

S. R. Abhishek Sharma, D. R. (2015). Detection of pneumonia clouds in chest x-ray using image processing approach. Institute for Plasma Research, HBNI Bhat, Gandhinagar,.

Salud, O. M. (2016). Neumonía. Retrieved from http://www.who.int/es/news-room/factsheets/detail/pneumonia

Sema Candemir, S. J. (2014). Lung segmentation in chest radiographs using anatomical atlases with nonrigid registration. IEEE TRANSACTIONSON MEDICAL IMAGING.

Shijin Kumar P.S, D. V. (2017). Extraction of Texture Features using GLCM and Shape Features using Connected Regions. International Journal of Engineering and Technology (IJET).

Xianghong Gu, L. P. (2017). Classification of bacterial and viral childhood pneumoniausingdeeplearninginchestradiography. Sun Yatsen University, Guangzhou.

ISSN-On line 2410-4191

Article **ECORFAN-Journal Bolivia**
December 2019 Vol.6 No.11 17-19

Carbon nanospheres as an electrode material for electroadsorption of Cu (II)

Las nanoesferas de carbono como material de electrodo para la electroadsorción de Cu (II)

KASHINA, Svetlana[1]†, BALLEZA, Marco[2], JACOBO-AZUARA, Araceli[1], GALINDO-GONZÁLEZ, Rosario[3]*

[1]*University of Guanajuato, Natural and Exact Sciences division, Department of Chemistry*
[2]*University of Guanajuato, Science and Engineering division, Department of Physics*
[3]*CONACYT cathedra in University of Guanajuato, Natural and Exact Sciences division*

ID 1st Author: *Svetlana, Kashina* / **ORC ID:** 0000-0003-4277-2060, **CVU CONACYT ID:** 516653

ID 1st Coauthor: *Marco, Balleza* / **ORC ID**: 0000-0002-3246-0277, **CVU CONACYT ID:** 406536

ID 2nd Coauthor: *Araceli, Jacobo-Azuara* / **ORC ID**: 0000-0003-0967-1858, **CVU CONACYT ID:** 104385

ID 3rd Coauthor: *Rosario, Galindo-González* / **ORC ID:** 0000-0002-3612-1555, **CVU CONACYT ID:** 223987

DOI: 10.35429/EJB.2019.11.6.17.19 Received: July 09, 2019; Accepted: September 23, 2019

Abstract

Objectives. Contamination with heavy metals has augmented in last decades due to several factors. So, scientific community has a challenge to develop new and more efficient methods for contaminants removal. Electroadsorption is one of investigated techniques with promising results. The main challenge with this technique is determination of optimal parameters, such as electrode material, time and conditions of adsorption. Material for electrode for electroadsorption must fulfil some criteria: high electroactive area, low electrical resistance and environmental compatibility. For that reason, our research group decided to synthetize a set of new carbon materials with high surface area and features than make them interesting to test them as an electrode material. Methodology. 3 carbon materials were synthetized by sol-gel method using different time and temperature conditions. All materials were characterized by scanning electron microscopy and other techniques. FTO glasses were modified with synthetized materials separately. Electroadsorption of Cu (II) was conducted at room temperature. Contribution. In this work we demonstrate an easy synthesis of 3 carbonaceous materials with high surface area capable to remove Cu (II) from water solution by electroadsorption.

Carbone nanospheres, Electroadsorption, Copper

Resumen

Objectivos. La contaminación con metales pesados ha aumentado debido a varios factores. Por lo tanto, la comunidad científica tiene el desafío de desarrollar métodos nuevos y eficientes para la eliminación de contaminantes. La electroadsorción es una de las técnicas con resultados prometedores. El desafío con esta técnica es la determinación de parámetros óptimos, como el material del electrodo y las condiciones de adsorción. El material de electrodo para la electroadsorción debe cumplir con algunos criterios: alta área electroactiva, baja resistencia y compatibilidad ambiental. En el grupo de trabajo se sintetizan nuevos materiales de carbono con características que los hacen interesantes para probarlos como material de electrodo. Metodología. Se sintetizaron 3 materiales de carbono mediante el método sol-gel utilizando diferentes condiciones de tiempo y temperatura. Todos los materiales se caracterizaron mediante microscopía electrónica de barrido y otras técnicas. Los vidrios FTO fueron modificados con materiales sintetizados. La electro-absorción de Cu (II) se realizó a temperatura ambiente. Contribución. La síntesis del material es sencilla, de bajo costo y amigable con el ambiente. Se muestran resultados para 3 materiales carbonosos con un área de superficie alta y capaz de remover Cu (II) de una solución acuosa mediante electro absorción.

Nanoesferas de carbono, Electroadsroción, Cobre

Citation: KASHINA, Svetlana, BALLEZA, Marco, JACOBO-AZUARA, Araceli, GALINDO-GONZÁLEZ, Rosario. Carbon nanospheres as an electrode material for electroadsorption of Cu (II). ECORFAN Journal-Bolivia 2019. 6-11: 17-19

* Correspondence to Author (email: galindorosario@gmail.com)
† Researcher contributing as first author.

Introduction

Environmental contamination with heavy metals due to variety of factors is a great problem. This contamination causes negative effect of ecosystems and human health. Copper intoxication is relatively rare condition, but its incidence have augmented in recent years because of the increase of copper concentration in waste waters.

Conventional methods such as active mud formation and precipitation of metals are not good strategy for copper removal, because the majority of copper salts are soluble in water. Electroadsorption may be the best option because its low cost and simple equipment.

The main challenge with this method is optimization of parameters of the process, such as material for electrodes, time, temperature and others.

Electrode material must meet some criteria: it should present high active area, los resistance to electric current and be environmentally friendly.

Carbon materials meet some specified criteria, but usually lack high surface area. To solve this problem, nanometric forms of carbon are developed.

Carbon nanospheres are relatively new form of carbon, and it possesses high surface area. Carbon nanospheres can be produced by variety of methods, but sol-gel synthesis is one of the best options due to scalability and controllability of the process.

Sol-gel synthesis of carbon nanospheres was described by Liu a al in 2011. It involves several steps, including gel formation y maturation for several hours. This process is time and energy consuming, so it is not easily applicable in industry.

For his reason, our research group decided to investigate an influence of reduction of time of synthesis and different temperature conditions on properties of resulted materials. Also, synthetized carbon nanospheres were assessed as electrode materials for Cu (II) electroadsorption.

Methodology

Synthesis. Carbone nanospheres were synthetized using methodology described by Liu et al in 2011 with some modifications. First polymeric spheres were produced by sol-gel process. Resorcinol was dissolved in mixture of water, ethanol and ammonium as a catalyst. Then formaldehyde was added drop by drop. Resulted mixture was left in stirring conditions for different time and under different temperature. After that, solid phase was separated by centrifugation, washed with water and ethanol, and dried overnight at 100 °C. Dry powder was carbonized separately in tubular oven at 900 °C for 3 h. Black material was recollected from the oven and named as SG-1, SG-2 and SG-3. General scheme of synthesis is presented in figure 1.

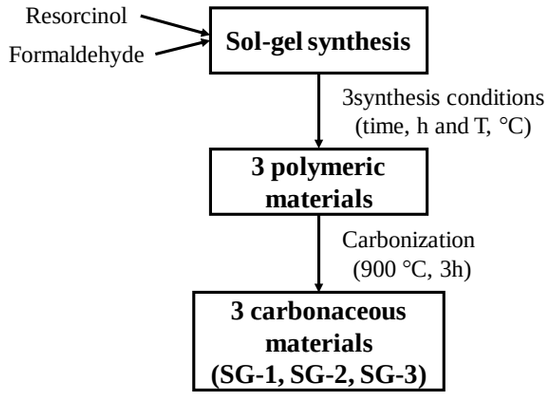

Figure 1 General scheme of synthesis of carbon nanospheres

Characterization. Scanning electron microscopy was performed for all 3 materials. Also, materials were characterized by FTIR an RAMAN spectroscopy. Surface area of materials was assessed by nitrogen adsorption-desorption.

Cu (II) removal. Electroadsorption was performed in neutral water solution of 20 ppm of Cu (II). FTO covered glasses were modified with carbon materials and used as electrodes. 2V constant voltage electrical current was applied to the system for 1-12 h. Percentage of Cu (II) removal was calculated as follows:

$$\%\ of\ removal = \frac{(Inicial\ concentration - final\ concentration}{inicial\ concentration} * 100\% \quad (1)$$

KASHINA, Svetlana, BALLEZA, Marco, JACOBO-AZUARA, Araceli, GALINDO-GONZÁLEZ, Rosario. Carbon nanospheres as an electrode material for electroadsorption of Cu (II). ECORFAN Journal-Bolivia. 2019.

Results

3 carbonaceous materials were synthetized. Scanning electron microscopy have shown that particles of all 3 materials present perfectly spherical shapes with 700 nm diameter, approximately.

FTIR spectra for all materials did not reveal peaks corresponding to any functional group, that was expected due to high temperature of carbonization. RAMAN spectra shown 2 peaks: G band at 1590 cm^{-1} than corresponds to sp^2 configuration and D band at 1310 cm^{-1} that is typical for amorphous carbon. So, all three synthetized materials are carbon nanospheres without significant number of functional groups and are not completely amorphous.

Results of physisorption of nitrogen have shown that materials possess specific surface area of approximately 440 m^2/g and are microporous.

Electroactive coverage prepared from materials separately have shown good adherence to FTIO covered glasses and did not detached from the surface during electroadsorption process. After desired time of adsorption was achieved, accumulation of metallic copper on the surface of electrodes was visible.

Table 1 comprises percentages of removal of Cu (II) from water solution. For all studied materials removal of approximately 30% of initial concentration was achieved after 12 h of the process.

Conclusions

Carbon nanospheres were synthetized avoiding gel maturation step without loss of shape and specific surface area. This omission allows to reduce time and cost of mass scale production of these materials. Also, synthetized materials were evaluated as electrode material for electrochemical removal of Cu (II) with acceptable results.

Functionalization of synthetized materials with different methods should be assessed in order to improve performance in electroadsorption.

Time of Electroadsorption (h)	Cu (II) removal (%) SG-1	SG-2	SG-3
1	9	18	5
2	15	21	12
3	15	21	12
4	18	24	14
5	18	24	16
6	18	27	16
7	21	27	19
8	24	27	19
9	24	27	21
10	27	30	26
11	27	30	26
12	30	33	28

Table 1 Removal of Cu (II) from water solution by electroadsorption

References

Bergmann, C. P., & Machado, F. M. (Eds.). (2015). Carbon nanomaterials as adsorbents for environmental and biological applications (pp. 1-122). Berlin: Springer.

Liu, J., Qiao, S. Z., Liu, H., Chen, J., Orpe, A., Zhao, D., & Lu, G. Q. (2011). Extension of the Stöber method to the preparation of monodisperse resorcinol–formaldehyde resin polymer and carbon spheres. Angewandte Chemie, 123(26), 6069-6073.

ISSN-On line 2410-4191

KASHINA, Svetlana, BALLEZA, Marco, JACOBO-AZUARA, Araceli, GALINDO-GONZÁLEZ, Rosario. Carbon nanospheres as an electrode material for electroadsorption of Cu (II). ECORFAN Journal-Bolivia. 2019.

Article **ECORFAN-Journal Bolivia**
December 2019 Vol.6 No.11 20-29

Proposed protocol with transcutaneous electrical nerve stimulation for the treatment of non-specific chronic low back pain

Propuesta de protocolo con estimulación nerviosa eléctrica transcutánea para el tratamiento del dolor lumbar crónico inespecífico

CORONA-BRISEÑO, Agustin†*

Universidad del Futbol y Ciencias del Deporte, San Agustín Tlaxiaca, Hidalgo, México.

ID 1st Author: *Agustin, Corona-Briseño* / **ORC ID:** 0000-0003-2954-5605

DOI: 10.35429/EJB.2019.11.6.20.29 Received: September 09, 2019; Accepted: November 04, 2019

Abstract

The low back pain is defined as pain or discomfort in an area around the upper portion of T12 and bottom of the gluteal fold, with functional limitation. It is the second most frequent cause of medical consultation at first care level. Objective: propose a protocol through electrotherapy utilizing transcutaneous electrical nerve stimulation (TENS) for the treatment of nonspecific chronic low back pain; It seeks to exemplify in a clear and concise method the type of frequency, pulse duration, intensity, placement of the electrodes, as well as duration and periodicity of the sessions to obtain the desired analgesic effect. Methodology: Quantitative type, non-experimental, retrospective, transversal and descriptive. Contribution: The application of Transcutaneous Electrical Nerve Stimulation in high and low frequency in the same session is effective in the treatment of nonspecific chronic low back pain because the lumbar mobility increases, the intensity of the pain decreases and therefore the degree of disability of patients.

Nonspecific low back pain, Protocol, TENS

Resumen

La lumbalgia se define como dolor o malestar en un área alrededor de la porción superior de T12 e inferior al pliegue de los glúteos, junto con limitación funcional. Es la segunda causa más frecuente de consulta médica en el primer nivel de atención. Objetivo: proponer un protocolo mediante electroterapia empleando estimulación nerviosa eléctrica transcutánea (TENS) para el tratamiento del dolor lumbar crónico inespecífico; se busca ejemplificar de forma clara y concisa el tipo de frecuencia, duración de pulso, intensidad, colocación de los electrodos, así como la duración y periocidad de las sesiones para obtener el efecto analgésico deseado. Metodología: Tipo cuantitativo, no experimental, retrospectivo, transversal y descriptivo. Contribución: La aplicación de Estimulación Nerviosa Eléctrica Transcutánea de alta y baja frecuencia en una misma sesión es eficaz en el tratamiento del dolor lumbar crónico inespecífico ya que aumenta la movilidad lumbar, disminuye la intensidad del dolor y por ende el grado de incapacidad de los pacientes.

Dolor lumbar inespecífico, Protocolo, TENS

Citation: CORONA-BRISEÑO, Agustin. Proposed protocol with transcutaneous electrical nerve stimulation for the treatment of non-specific chronic low back pain. ECORFAN Journal-Bolivia. 2019. 6-11: 20-29.

* Correspondence to Author (aguscorona10@gmail.com)
† Researcher contributing as first author.

Introduction

Low back pain is the second most frequent cause of medical consultation in the first level of care, between 60 and 80% of the population will experience this problem at some time in their life, which will condition 40% of all work absences, decreasing the productivity of those affected. The prevalence of this health problem is increasing by 11.4% per year, so it is a pathology that occurs very often in health services.

Low back pain is defined as pain or discomfort in an area around the upper portion of T12 and lower than the buttock fold, along with functional limitation. This concept does not apply to a specific low back pain and is independent of the cause that gave rise to it. (1)

Three types of low back pain are distinguished based on the time of evolution:

1. Acute low back pain: lumbar pain that is less than six weeks old.

2. Subacute low back pain: if pain in the lower back remains between six and twelve weeks.

3. Chronic low back pain: when low back pain persists for more than 12 weeks.

According to the possible origin of low back pain, we can also classify it into:

1. Non-specific low back pain: this is the pain in which there is no apparent cause.

2. Low back pain associated with radiculopathy: that discomfort with neurological involvement that radiates to one of the two lower extremities.

3. Secondary low back pain: the main causes of this type of pain would be infections, tumors, inflammatory diseases such as ankylosing spondylitis, fractures, cauda equina syndrome, among others. (2)

The treatment of low back pain consists in reducing pain, improving functionality and quality of life, as well as avoiding recurrences. Pharmacological treatment should be based on the analgesic ladder of the World Health Organization (WHO).

Various groups of analgesics are used, from non-steroidal anti-inflammatory drugs (NSAIDs), muscle relaxants, antidepressants and local anesthetics that have demonstrated efficacy for such ailment. In relation to non-pharmacological treatment, the main goal is to try to reduce or eliminate pain, in addition to ensuring the return to daily activities and work. There are several studies that report a significant clinical improvement with rehabilitation exercises, however, few studies prove its effectiveness in alternative intervention methods such as: low intensity laser, transcutaneous electrical nerve stimulation, thermotherapy, lumbar traction and / or massage leaving its effectiveness is in doubt, so it is necessary to demonstrate that treatment alternatives improve functionality in addition to reducing the risk of polypharmacy or complications. (3)

The TENS application has a wide variety of parameters such as electrode placement, waveform, frequency, pulse width, current intensity, as well as the duration and frequency of the sessions. The optimization of these parameters is essential to achieve the desired therapeutic effects, however, existing studies have great variability in the use of these parameters, which is one of the reasons why the effectiveness of TENS has been controversial. (4).

When applying TENS, patients can develop tolerance to stimulation, similar to the tolerance that develops to opiates. Tolerance determines the need for higher intervention doses to achieve the same effect. Patients may develop TENS tolerance from the fourth or fifth day of stimulation. It has been shown that frequency modulations, similar to those used to prevent accommodation, delay tolerance to TENS-induced analgesia. (5)

The objective of this work is to propose a protocol by electrotherapy using transcutaneous electrical nerve stimulation (TENS) for the treatment of nonspecific chronic low back pain. It seeks to exemplify in a clear and concise manner the type of frequency, pulse duration, intensity, placement of the electrodes, as well as the duration and periodicity of the sessions to obtain the desired analgesic effect.

ISSN-On line: 2410-4191

Annex to the aforementioned, another purpose is to clarify whether the phenomenon of TENS tolerance exists or not, as well as to demonstrate the impact of said therapeutic current in the short and long term in the treatment of chronic low back pain since up to now its utility in this condition is controversial.

Central awareness

When a tissue is damaged and the pain persists for a few days, mechanisms of adaptation of the nociceptors and the nociceptive response to damage occur. This process is called primary hyperalgesia or peripheral sensitization and represents a protective action of the human body against possible future damage. Secondary hyperalgesia or central sensitization (SC) refers to the process of increasing the response in the dorsal horn, located in the nociception processing segments. Peripheral sensitization is temporary, SC is a process that encompasses the central nervous system.

Central hyperexcitability is responsible for the amplification of the nociceptive afferent signal that arrives from the periphery, which produces structural modifications such as alterations in genetic regulation and causes the death of inhibitory neurons. Other mechanisms involved in CS are: malfunction of descending pain inhibitory mechanisms and an increase intemporal summation.

The descending pain system is controlled by a correct balance between the inhibitory descending system and the facilitating descending system. A reduction in the control of the descending inhibitory system results in a greater vulnerability of the entire neuroaxis to pain as a result of a generalized induction to hyperalgesia.

Temporal summation is a measure of central mechanisms that is triggered by the application of a sequence of stimuli with the same intensity where there is an increase in painful sensation. In the case of CS this mechanism is altered and results in a facilitation of said summation, which has been observed in patients with chronic musculoskeletal pain.

Transcutaneous electrical nerve stimulation (TENS) is frequently used in patients with chronic pain, its mechanism of action activates the descending inhibitory system, which in turn is activated by the gray periacueductal substance and the ventromedial rostral ganglion of the medulla. Therefore, the TENS current is involved in the mechanisms of SC. (6)

TENS high frequency

Also known as conventional TENS, it uses two-phase pulses of short duration (50-80 microseconds) and high frequency (100-150 pulses per second) with amplitude that produces a comfortable sensation without muscle contraction.

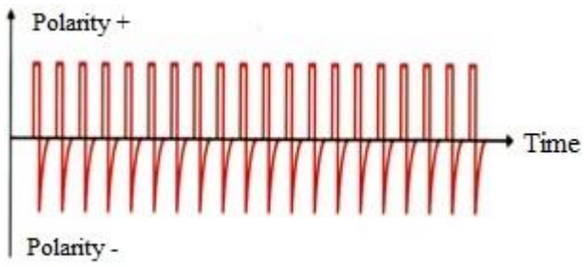

Figure 1 TENS high frequency current
Source: Cameron, M. (2019). Physical agents in rehabilitation. Evidence based practice. Barcelona: ELSEVIER

Sensitive electrical stimulation can control pain by activating the non-nociceptor Aβ (A beta) nerves, which inhibits the transmission of harmful signals at the level of the spinal cord. When Aβ activity increases, pain perception is reduced.

Conventional TENS can interrupt the pain-spasm-pain cycle once the stimulation subsides. Pain decreases directly through electrical stimulation, which indirectly reduces muscle spasm, further mitigating pain. (5)

High frequency TENS (TAF) increases the concentration of β-endorphins in the bloodstream and cerebrospinal fluid, and enkephalin methionine only in the cerebrospinal fluid. The analgesia produced prevents the reduction of hyperalgesia by blocking opioid receptors in the ventromedial rostral medulla (MRV) or spinal cord, or blocks synaptic transmission in the ventrolateral gray periacueductal substance (GSP).

ISSN-On line: 2410-4191

The reduction of hyperalgesia produced by TAF is avoided by blocking the M1 and M3 muscarinic receptors, and the GABA receptors in the spinal cord. However, blocking serotonin or noradrenergic receptors in the spinal cord has no effect on the reversal of hyperalgesia caused by TAF.

TAF produces analgesia by activating endogenous inhibitory mechanisms in the central nervous system that involve opioid GABA and muscarinic receptors. (7)

Opioid release

Transcutaneous electrical nerve stimulation can control pain by stimulating the production and release of endorphins and encephalin. These substances known as endogenous opioids act similarly to morphine and modulate the perception of pain by binding to opioid receptors, which activate the descending inhibitory pathways that involve non-opioid systems (serotonin). (5)

TENS low frequency

It uses a frequency of 2 to 10 pulses per second, long duration amplitude: 200 to 300 μs (microseconds) with sufficient intensity to produce a motor contraction. Repetitive stimulation of motor nerves increases the production and release of endogenous opiates and increases their ability to bind opioid receptors.

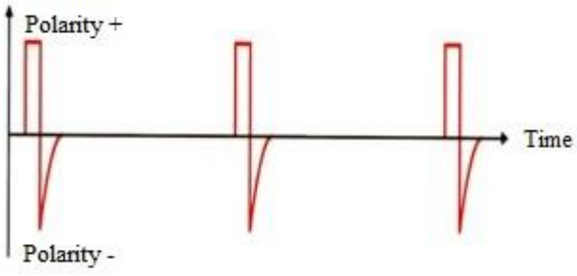

Figure 2 TENS current low frequency
Source: Cameron, M. (2019). Physical agents in rehabilitation. Evidence based practice. Barcelona: ELSEVIER

After a session with low frequency TENS an analgesic effect is exerted for 4-5 hours since this is the average life time of the released endogenous opioids.

Electrical stimulation should not exceed 45 minutes per session because prolonged muscle contraction can lead to late-onset myalgias. (5)

The reduction of hyperalgesia by low frequency TENS (TBF) is avoided by blocking the opioid receptors μ in the spinal cord or MRV and by synaptic transmission in the ventrolateral GSP. In addition, the reduction of hyperalgesia due to TBF is avoided by blocking serotonin 5-HT2A and 5-HT3, GABA and M1 and M3 muscarinic receptors in the spinal cord, which is associated with increased serotonin release. TBF does not produce analgesia in opioid-tolerant people but TAF does, therefore, TBF uses classical descending inhibitory pathways that include the activating opioid SGP-MRV, GABA, serotonin and muscarinic receptors to reduce the activity of the horn neuron dorsal and subsequent pain. (7)

Reduction of central excitability

Both TAF and TBF reduce the activity of dorsal horn neurons. In individuals with peripheral inflammation or neuropathic pain, the increased activity of dorsal horn neurons to harmful and harmless stimuli is reduced by both TAF and TBF. At the same time there is a reduction in both primary and secondary hyperalgesia with TAF and TBF, in addition there is a reduction in pain thresholds by pressure not only at the stimulation site, but also at sites outside the application area, implying a reduction of central excitability.

TAF also reduces the sensitization of central neurons and the release of neurotransmitters that excite glutamate and substance P in the spinal cord's dorsal horn in individuals with inflammation. The reduction of glutamate is avoided by blocking δ opioid receptors, therefore, a consequence of the activation of the inhibitory pathways exerted by TENS is to reduce the excitation and consequent sensitization of neurons in the spinal cord. Both TAF and TBF have effects at the stimulation site, TAF reduces substance P, which increases in the neurons of the dorsal root ganglia after a tissue injury. Blocking peripheral opioid receptors prevents analgesia caused by TBF but not by TAF. Therefore, TENS can also alter the excitability of peripheral nociceptors to reduce afferent entry to the central nervous system. (7)

ISSN-On line: 2410-4191

Most used scales for pain assessment

Defining pain and doing it in such a way that it has a unanimous acceptance is complex, since it is an individual and subjective experience, to which is attached the fact that there is no scientific method that makes it measurable. To evaluate it, instruments are used that are easily understandable, of minimal effort for the patient, and that demonstrate reliability and validity.

Although all pain scoring scales are valid, reliable and appropriate for use in clinical practice, the Visual Analog Scale (VAS) has more practical difficulties than the Verbal Score Scale (CVD) or the Numeric Scale (EN). For general purposes, the EN has a good sensitivity and generates data that can be statistically analyzed.

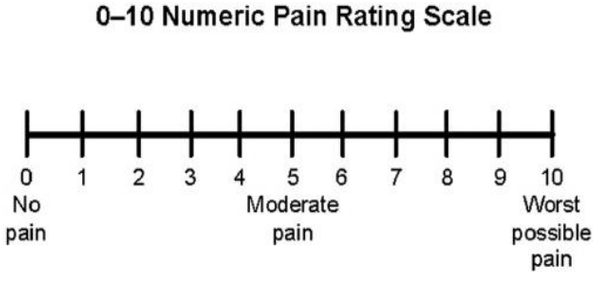

Figure 3 Numerical scale
Source: Swartz, M. H. Treaty of Semiology. History and exploration. Seventh edition. Barcelona 2015

The EN is a numbered range from 0 to 10, where 0 is the absence of pain and 10 is the greatest intensity of it, the patient selects the number that best assesses the intensity of the symptom. (8)

Oswestry low back pain disability scale

It is a self-applied questionnaire consisting of 10 questions concerning activities of daily living that can be interrupted or altered by low back pain. Each question has six possible answers that progressively describe a greater degree of difficulty of the activity. The first question refers to the intensity of pain, specifying in different options the answer to taking painkillers. The remaining items include basic activities of daily living that can be affected by pain (personal care, weight lifting, walking, sitting, standing, sleeping, sexual activity, social life and traveling). It is the most used and recommended scale.

The answers are scored from zero to five, giving a maximum score of 50, the total points are multiplied by two and expressed as a percentage. The results are cataloged as follows: no dysfunction (0%), minimal dysfunction (1% to 20%), moderate dysfunction (21% to 40%), severe dysfunction (41% to 60%) and disability (greater than 61%). (9)

Lumbar flexion assessment

During the life cycle people develop arcs of movement that allow them to be integrated into mechanical tasks of the locomotor system, including those related to the lumbar spine flexion, which involves multiple morphological elements among which are intervertebrales discs, which They allow moderate movements thanks to their flexibility and increased intradiscal pressure. In addition, the type of joints, the elasticity of tissues, tendons, ligaments and the length of the muscles can affect lumbar mobility. (10)

Quantification of spinal mobility is a beneficial component in physiotherapeutic assessment for people experiencing limited spinal mobility as a result of disorders or injuries in the spine. (eleven). In a study evaluating the inter-evaluative reliability and validity of common clinical trials that measure the range of lumbar movement, it was found that the modified Schober maneuver could be the best criterion for measuring the range of lumbar flexion. (10).

Modified Schober Test

Technique used in the exploration of lumbar mobility, which measures the increase in distance (in centimeters) between 2 defined points on the lower back, which excludes the influence of the hip, pelvis and hamstring joints, which gives excellent inter-evaluation reliability, its use is widely recommended in clinical practice. (10).

A mark is made on the midline at the level of the posterior superior iliac spine (i.e., S2), then a point 5 cm below and 10 cm above that mark is indicated. The distance between the three points is measured, then the patient is asked to flex forward and the distance is measured again. (11)

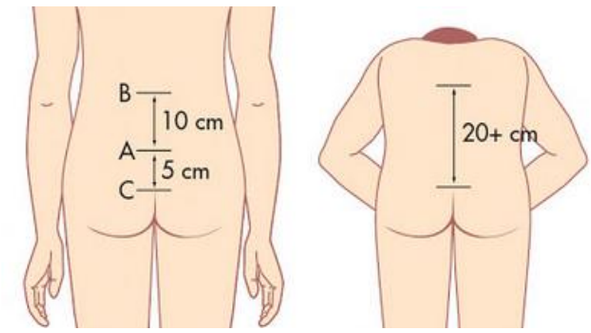

Figure 4 Schober test modified. (A) point between both EIPS; (B) upper point; (C) bottom point
Source: Talley, N. J., & O'Connor, S. (2013). Clinical examination: a systematic guide to physical diagnosis. Elsevier Health Sciences

The measurement difference between the upper and lower points is an indication of the magnitude of flexion in the lumbar spine. It is expected that, with trunk flexion, the second measurement will increase by at least 5 centimeters compared to the first. If this does not occur, the patient is considered to have a limitation for lumbar spine flexion. (12).

Material and methods

Twenty people with low back pain were included, of which 15 met the inclusion criteria: low back pain with 3 or more months of evolution and signed informed consent. Patients with unstable arrhythmia, cardiac pacemaker on demand, implantable defibrillator, deterioration of mental status, open wounds in the lumbar area, postoperative lumbar spine carriers carrying some type of electrical conductive surgical material (plates, nails, screws) were excluded, sensitivity impairment, malignant tumors or pregnancy. The materials used for the application of the protocol were: a HomeCare® model M012A 3-section portable physiotherapy stretcher, an Oswestry low back pain scale questionnaire, a Fith by HERGOM® model R12 medical measuring tape, a permanent marker BIC® Marking ™ fine point, a Globus® GENESY 3000 electrostimulator and four 4x8 cm rectangular KHG-CM4080 self-adhesive electrodes with cable and PVC coated connector, carbon conductive plate.

Protocol Application

At the beginning of the session, the patient is asked to assess the intensity of his low back pain according to the numerical scale, then the Oswestry questionnaire is delivered and its filling is requested.

Subsequently, with the patient standing, the marks marking the modified Schober test are marked with the permanent BIC® Marking ™ marker, then the Fith by HERGOM® model R12 medical measuring tape is taken, simultaneously, while the patient performs a trunk flexion with the knees extended trying to touch the floor with the fingers, the therapist measures the distance between the upper and lower point previously indicated and records the result.

Then, the patient is placed prone on the stretcher for portable physiotherapy of 3 sections brand HomeCare® model M012A, then, with the lumbar area discovered and his previous asepsis, the first rectangular self-adhesive electrode KHG-CM4080 of 4x8 cm is placed horizontally in the upper portion of T12 at 3 cm lateral to the midline, the second electrode is placed at the level of the posterior iliac spine, that is S2, also horizontally at 3 cm lateral to the midline, both of the right side of the spine. Then, the two remaining electrodes repeat the same placement of the previous ones, now on the left side of the column.

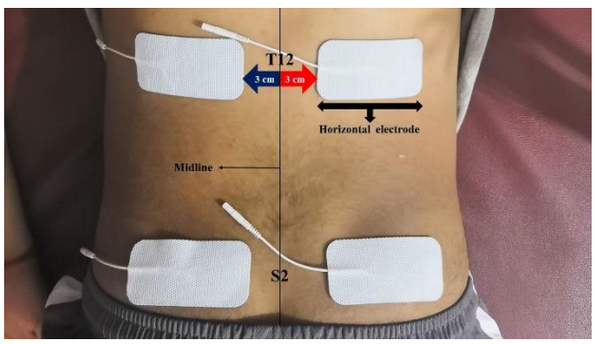

Figure 5 Placement of the self-adhesive electrodes
Source: Self Made

Subsequently, channel 1 and 2 of the Globus® GENESY 3000 electrostimulator are taken, the positive (+) pole of channel 1 is placed on the upper right electrode, the cathode (-) of the same channel is placed longitudinally on the lower electrode straight.

The polarity of channel 2 of the electrostimulator is placed equally on the left side: upper (+) anode, lower (-) cathode.

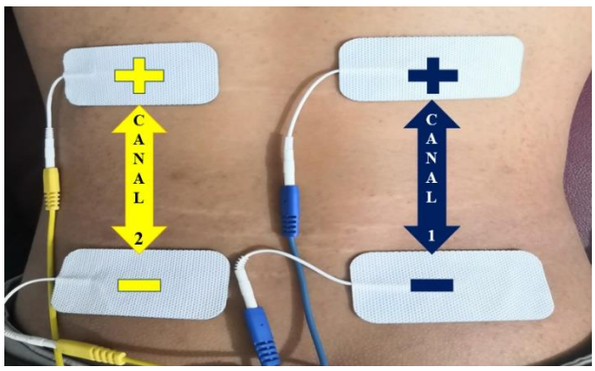

Figure 6 Polarity placement: the blue wire is channel 1 of the electrostimulator and the yellow one is channel 2
Source: Self Made

Then, in the Globus® GENESY 3000 electrostimulator, the high frequency TENS current is selected at 120 Hz (pulses per second), amplitude of 80 µs (microseconds), maximum intensity tolerated by the patient without generating pain for 20 minutes. Then, once the high frequency TENS stimulation ceases, in the same position of the patient and placement of both electrodes and electrostimulator polarity, low frequency TENS is applied at 3 Hz (pulses per second), amplitude of 250 µs (microseconds), sensory intensity for 10 minutes.

Figure 7 Programming of the electrostimulator: TENS high frequency
Source: Self Made

Figure 8 Programming of the electrostimulator: Low frequency TENS
Source: Self Made

The treatment was placed for 30 minutes, once a week for 3 months (14 weeks). The Oswestry questionnaire and the modified Schober test were applied prior to the start of the first session and at the end of the fourteenth treatment session. Regarding the perception of low back pain, before and after each treatment the patient was asked to indicate its intensity according to the numerical scale.

Methodology

Quantitative, non-experimental, retrospective, cross-sectional and descriptive type in patients with nonspecific chronic low back pain who attended the Physical Therapy and Rehabilitation service in the period between May 20 and August 22, 2019.

Results

A total of 15 people participated, in which the male sex prevailed with 53.3% having 8 participants for 46.6% of the female sex (7 participants); they had an age range of 19 to 58 years, the average age of the patients was 40.6 years.

General patient data		
	Total	Percentage
Men	8	53.3%
Women	7	46.6%
Average age: 40.6 years		

Table 1 General data
Source: Self Made

Regarding the classification of low back pain according to its possible origin, of the 15 patients who participated 11 (73.3%) suffered from non-specific low back pain, 2 (13.3%) low back pain associated with radiculopathy and the remaining 2 (13.3%) had low back pain secondary.

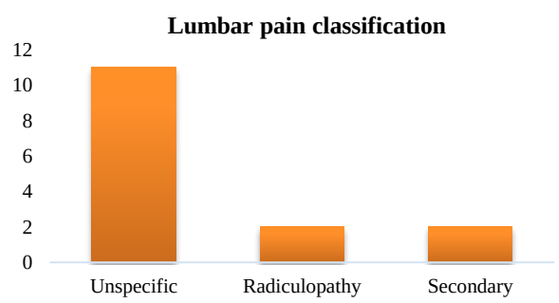

Graphic 1 Classification of low back pain according to its possible origin
Source: Self Made

Regarding the Oswestry low back pain disability scale, the questionnaire delivered prior to the first treatment session showed an average disability percentage of 21.73%, at that time the highest record was 50% and the lowest was 4 %. Three months later, at the end of the fourteenth treatment session, the highest percentage of disability was 10% and the lowest was 4%, while the average was 3.6%. That is, after the study, disability due to low back pain decreased on average 81.1% (table 2).

Oswestry low back pain disability scale			
	Initial percentage	**Final percentage**	**Improvement**
1	8%	0%	100%
2	4%	4%	0%
3	28%	4%	85.7%
4	20%	8%	60%
5	32%	2%	93.7%
6	26%	6%	76.9%
7	50%	10%	80%
8	6%	0%	100%
9	30%	10%	66.6%
10	18%	0%	100%
11	38%	0%	100%
12	6%	0%	100%
13	20%	4%	80%
14	24%	6%	75%
15	16%	0%	100%
Total	21.7%	3.6%	81.1%

Table 2 Percentages of the Oswestry low back pain disability scale
Source: Self Made

Regarding the modified Schober test, it was applied to each of the 15 participants prior to the first treatment session, the maximum registered mark was 19.8 cm, while the minimum was 17.4 cm; The average of the test was 18.84 cm. Subsequently, once the last treatment session was completed, the minimum level recorded was 19.6 cm and the maximum was 23.9 cm; The average showed a result of 21.75 cm. That is, between the first and fourteenth treatment session, on average, there was an increase in lumbar mobility of 2.9 cm (table 3).

Modified Schober Test			
	Initial Mark (cm)	**Final mark (cm)**	**Increase in cm**
1	19.2 cm	20 cm	0.8 cm
2	19.8 cm	21.7 cm	1.9 cm
3	17.8 cm	20.7 cm	2.9 cm
4	19.2 cm	23.7 cm	4.5 cm
5	18 cm	21.2 cm	3.2 cm
6	19.1 cm	23 cm	3.9 cm
7	17.4 cm	19.6 cm	2.2 cm
8	19.8 cm	21 cm	1.2 cm
9	18.5 cm	21.5 cm	3 cm
10	19.3 cm	22.6 cm	3.3 cm
11	18.3 cm	21 cm	2.7 cm
12	19.1 cm	23.9 cm	4.8 cm
13	19.3 cm	22.8 cm	3.5 cm
14	18.9 cm	21.4 cm	2.5 cm
15	19 cm	22.2 cm	3.2 cm
Average	**18.84 cm**	**21.75 cm**	**2.9 cm**

Table 3 Records of the modified Schober test
Source: Self Made

Regarding the perception of low back pain, before and after each treatment session, each of the 15 participants was asked to indicate the intensity of the same according to the numerical scale. Prior to the start of the study, low back pain averaged an intensity of 7.1 / 10; seven weeks later, in the middle of the study, pain perception decreased and averaged an intensity of 3.3 / 10; finally, after the fourteenth treatment session, the intensity of low back pain showed an average of 1.3 / 10 (graphic 2).

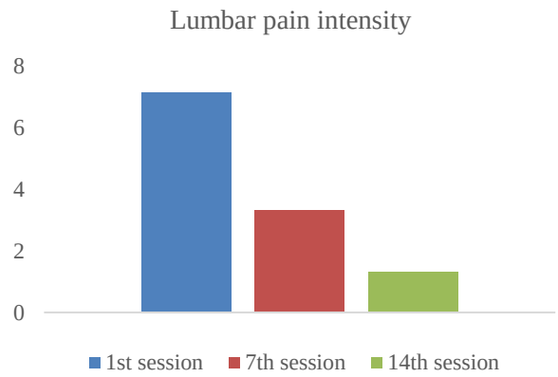

Graphic 2 Records of the intensity of low back pain according to the numerical scale
Source: Self Made

Before the start of the study, each participant indicated the intensity of low back pain, based on the numerical scale, at that time the highest record was 10/10, while the lowest was 5/10, the average was 7.1 / 10. For half of the study, that is, seven sessions later, the maximum recorded intensity of low back pain was 6/10 and the minimum was 1/10; the patient with the lowest percentage of improvement registered an advance of 33.3%, while the one with the greatest progress showed an improvement of 80%. After 7 sessions, the perception of discomfort decreased on average 54.1% compared to the start of the study (table 4).

Lumbar pain intensity			
	First session	Seventh session	Percentage of improvement
1	8/10	4/10	50%
2	5/10	3/10	40%
3	9/10	4/10	55.5%
4	6/10	2/10	66.6%
5	8/10	3/10	62.5%
6	7/10	3/10	57.1%
7	10/10	6/10	40%
8	6/10	4/10	33.3%
9	9/10	6/10	33.3%
10	5/10	2/10	60%
11	9/10	3/10	66.6%
12	6/10	3/10	50%
13	6/10	2/10	66.6%
14	8/10	4/10	50%
15	5/10	1/10	80%
Average	**7.1**	**3.3**	**54.1%**

Table 4 Records of the intensity of low back pain between the first and seventh week according to the numerical scale
Source: Self Made

The perception of low back pain before and after the study decreased considerably, initially the average intensity of discomfort, according to the numerical scale, was located at 7.1 / 10, after three months (14 sessions) of treatment, low back pain averaged an intensity of 1.3 / 10. The 15 participants showed improvement, pain decreased between 50% and 100%, on average, the perception of discomfort dropped 82.9% compared to the start of the study (table 5).

Lumbar pain intensity before and after the study			
	First session	Last session	Percentage of improvement
1	8/10	0/10	100%
2	5/10	1/10	80%
3	9/10	3/10	66.6%
4	6/10	1/10	83.3%
5	8/10	1/10	87.5%
6	7/10	1/10	85.7%
7	10/10	5/10	50%
8	6/10	2/10	66.6%
9	9/10	3/10	66.6%
10	5/10	0/10	100%
11	9/10	0/10	100%
12	6/10	0/10	100%
13	6/10	1/10	83.3%
14	8/10	2/10	75%
15	5/10	0/10	100%
Average	**7.1**	**1.3**	**82.9%**

Table 5 Records of the intensity of low back pain at the beginning and end of the study according to the numerical scale
Source: Self Made

Conclusions

The application of high and low frequency Transcutaneous Electrical Nerve Stimulation in the same session is effective in the treatment of nonspecific chronic low back pain as it increases lumbar mobility, decreases the intensity of pain and therefore the degree of disability of patients.

TENS is useful for this condition in the short and long term, the phenomenon of tolerance to said therapeutic current was not evident.

References

Álvarez Araújo, N. (2016). Efectividad del tratamiento mediante la técnica músculo energía (MET) aplicada al psoas-ilíaco en el dolor lumbar crónico en taxistas.

Cameron, M. (2019). Agentes físicos en rehabilitación. Práctica basada en la evidencia. Barcelona: ELSEVIER.

Fernández-Tenorio, E., Serrano-Muñoz, D., Avendaño-Coy, J., & Gómez-Soriano, J. (2016). Estimulación eléctrica nerviosa transcutánea como tratamiento de la espasticidad: una revisión sistemática. Neurología.

Jiménez-Ávila, J. M., Rubio-Flores, E. N., González-Cisneros, A. C., Guzmán-Pantoja, J. E., & Gutiérrez-Román, E. A. (2018). Directrices en la aplicación de la guía de práctica clínica en la lumbalgia. Cirugía y Cirujanos, 86(1), 29-37.

Masselli, M. R., Fregones, C. E. P. T., de Faria, C. R. S., Bezerra, M. I. S., Junges, D., & Nishioka, T. H. (2017). Índice funcional de oswestry após cirurgia para descompressão de raízes nervosas. Fisioterapia em Movimento, 20(1).

Mojica, H. M. B., Parra, J. E. D., & Cortés, F. J. C. P. (2017). Variaciones del rango de flexión lumbar en una muestra poblacional sana de niños y niñas escolares caldenses (Colombia). Medicina, 39(3), 181-189.

Ortíz, F. (2016). Texto de medicina física y rehabilitación. Editorial El Manual Moderno Colombia SAS.

Serrano-Muñoz, D., Gómez-Soriano, J., Ávila-Martín, G., Galán-Arriero, I., Romero-Muñoz, L. M., Taylor, J. S., & Barriga-Martín, A. (2016). Sensibilización central al dolor en pacientes con síndrome del latigazo cervical: una revisión. Revista Latinoamericana de Cirugía Ortopédica, 1(3), 102-107.

Vance, C. G., Dailey, D. L., Rakel, B. A., & Sluka, K. A. (2014). Using TENS for pain control: the state of the evidence. Pain management, 4(3), 197-209.

Varangaonkar, V. C., Ganesan, S., & Kumar, K. V. (2015). The relationship between Lumbar range of motion with hamstring flexibility among 6-12 years children from South India: A cross-sectional study. International Journal of Health & Allied Sciences, 4(1), 23.

Vicente-Herrero, M. T., Delgado-Bueno, S., Bandrés-Moyá, F., & Capdevilla-García, L. (2018). Valoración del dolor. Revisión comparativa de escalas y cuestionarios. Revista de la Sociedad Española del Dolor, 25(4), 228-236.

Villanueva Estrada, E. M., Hernández Bedolla, I., & González Pedraza Avilés, A. (2015). Efectividad del tratamiento láser con ejercicio vs tens con ejercicio en la lumbalgia inespecífica. Revista Cubana de Medicina Física y Rehabilitación, 7(2), 116-123.

Article **ECORFAN-Journal Bolivia**
December 2019 Vol.6 No.11 30-34

Predictibility and aesthetics in the anterior sector

Previsibilidad y estética en el sector anterior

OROZCO-RODRIGUEZ, Rubén, ROSADO-VILA, Graciella, ZAPATA-MAY, Rafael and PINZON-SIERRA, Patricia

Universidad Autonoma de Campeche, Faculty of Odontology and Faculty of Nursing, San Francisco de Campeche, México

ID 1st Author: *Ruben, Orozco-Rodriguez* / **ORC ID**: 0000-0002-5425-0107

ID 1st Coauthor: *Graciella, Rosado-Vila* / **ORC ID**: 0000-0002-8688

ID 2nd Coauthor: *Rafael, Zapata-May* / **ORC ID**: 0000-0002-3750

ID 3rd Coauthor: *Patricia, Pinzon-Sierra* / **ORC ID**: 0000-0001-7842-9841

DOI: 10.35429/EJB.2019.11.6.30.34 Received: September 09, 2019; Accepted: December 30, 2019

Abstract

Introduction: Today the aesthetic demand in dentistry occupies the first places in terms of consultation needs in the dental office, that is why, as providers of dental health services, we are obliged to offer treatment options that meet standards of quality, functionality, aesthetics, predictability among other things and that are available to different social levels4. There are techniques that supported by elements such as Digital Smile Design (DSD) 9, wax up and mockup5 offer excellent, predictable aesthetic results, with the option of choosing different materials that are available to all our patients from composite resin to better than we find today; the porcelain clinical case: A 25-year-old female patient who goes to a dental office for teeth whitening, when diagnosing the case, the presence of diastema was observed in the upper centers, as well as anomalies regarding aesthetic smile parameters such as pigmentation, proportions , incisal edge line, among other things. Diagnostic waxing, mockup and photographs were performed to evaluate the result. The treatment plan consisted of 6 resin veneers made with the fluid resin injection technique through a transparent silicone matrix (Flow injection technique). RESULTS: The prognosis of the case is considered favorable, taking into account that the treatment with Resins is not definitive, however functional and aesthetic results were achieved properly. Conclusions: There are several treatment alternatives for the solution of aesthetic problems, which adapt to the possibilities of each patient, the mockup is a necessary tool for obtaining predictable treatments. The fluid resin injection technique is a good aesthetic and functional treatment, which sometimes does not require the minimum wear of the teeth to be treated.

Dental prosthesis, Oral health, Aesthetics

Resumen

Introducción: Hoy en día la demanda estética en odontología ocupa los primeros lugares en cuanto a necesidades de consulta en el consultorio dental, por lo que, como prestadores de servicios de salud dental, estamos obligados a ofrecer opciones de tratamiento que reúnan estándares de calidad, funcionalidad, estética, predictibilidad entre otras cosas y que estén al alcance de los distintos niveles sociales[4]. Existen técnicas que apoyadas por elementos como el Diseño Digital de Sonrisa (DSD)[9], el wax up y el mockup[5] ofrecen excelentes resultados estéticos predecibles, con la opción de elegir distintos materiales que estén al alcance de todos nuestros pacientes desde resina compuesta hasta lo mejor que encontramos hoy en día; la porcelana. Caso clínico: Paciente femenina de 25 años que acude a consulta odontológica por blanqueamiento dental, al realizar el diagnóstico del caso se observó la presencia de diastema en los centrales superiores, así como anomalías en cuanto a parámetros de sonrisa estéticos: como pigmentaciones, proporciones, línea del borde incisal, entre otras cosas. Se realizó encerado de diagnóstico, mockup y fotografías para evaluar el resultado. El plan de tratamiento constó de 6 carillas de resina, elaboradas con la técnica de inyección de resina fluida a través de una matriz de silicona transparente (Flow injection technique). Resultados: El pronóstico del caso se considera favorable, tomando en cuenta que el tratamiento con resinas no es definitivo, sin embargo los resultados funcionales y estéticos se lograron obtener adecuadamente. Conclusiones: el mockup es una herramienta necesaria para la obtención de tratamientos predecibles. La técnica de inyección de resina fluida es una buen tratamiento estético y funcional, que en ocasiones no requiere desgaste de los dientes a tratar.

Protesis dental, Salud oral, Estética

Citation: OROZCO-RODRIGUEZ, Rubén, ROSADO-VILA, Graciella, ZAPATA-MAY, Rafael and PINZON-SIERRA, Patricia. Predictibility and aesthetics in the anterior sector. ECORFAN Journal-Bolivia. 2019. 6-11: 30-34

† Researcher contributing as first author.

Introduction

The word aesthetic comes from the Greek "αìσθηΤΙΚός" which means "perception." The term aesthetics from an etymological point of view means, relative to a state of "sensitive" esthesia as the "no sensitivity" anesthesia counterpart. At present the term has been used as a study of beauty and its opposite ugliness[3]. Some authors mention that beauty can be divided into two dimensions: objective (admirable) and subjective (pleasant) beauty. Objective beauty implies that the object possesses properties that make it evidently commendable. Subjective beauty is loaded with value and is related to the tastes of the person who contemplates it. ” Contemporary dentistry techniques should help objective aesthetics for the orofacial complex, encompassing coherence, shape, structure, balance, color, function and dental exposure. You might think that the search for these aesthetic characteristics in the position of this or that dental organ is to look for characteristics of that objective “beauty”[3].

Today the aesthetic demand in dentistry occupies the first places in terms of consultation needs in the dental office, so, as providers of dental health services, we are obliged to offer treatment options that meet quality standards, functionality, aesthetics, predictability among other things and that are within reach of different social levels. Currently there are different options in terms of materials to offer our patients, there is no doubt that porcelain is a material for the rehabilitation of teeth that has advantages over others, but its Achilles heel is located in the cost as it remains high above compared to others such as composite resin, with which we can obtain excellent results if your treatment protocol is adequate; and in this way expand the range of possibilities to offer for our treatments and that are available to all people[4,2].The composite resin has been positioned as one of the materials of choice not only as a direct restoration material, in cases of dental surgery or reconstruction of teeth with root canal treatment, but also for its improved qualities over the years today Its use includes aesthetic functional prototypes and transient smile designs whose varied techniques for its realization have achieved very favorable results.[6,7]

At present, the use and use of auxiliaries is of paramount importance so that our treatments are predictable and thus be able to convince us of their reliability. The digital smile design (DSD) is a digital planning tool for aesthetic dentistry, in which the evaluation of the aesthetic relationship between teeth, gum, smile and face is obtained through digital lines and drawings that they are inserted in the patient's facial and intraoral photographs. The use of digital tools offers dentists and technicians a new perspective for diagnosis and treatment plan, facilitating and improving communication between the dentist, the technician and the patient9. Other auxiliary and no less important elements are wax up and mock up; The first is to develop an aesthetic solution from a plaster model of the patient using laboratory wax. However, aesthetic and functional benefits are limited.

From the aesthetic point of view, the wax allows to visualize the shape and position of the teeth in the planned restoration, but does not reproduce exactly the color and function of the teeth, for this it is necessary that the mock up comes into play, This is a preview model made with materials such as acrylic resin or composite resin. This technique allows a preview of the aesthetic result and, thus, plays an important role in the planning of treatment. The mock-up constitutes the phase after the waxing validation. In this step, the restoration model, previously validated in the plaster model, is adjusted in the patient's mouth. In this way, the waxing information can be transferred directly from the patient's model to the mouth. The "test" in the patient's mouth can be checked for aesthetic, functional and psychological aspects of the restoration. This last point is decisive in providing an important concept for patient acceptance.[5].

The injected fluid resin technique is a novel direct / indirect process that allows us to foreseeably reproduce a diagnostic waxing with composite resin restorations, by injecting it into the patient's natural teeth through a transparent silicone matrix. Clinical applications include emergency repair of fractured teeth and restorations, fabrication of provisional restorations, composite transition restorations (class III, IV, veneers)

ISSN-On line: 2410-4191

And pediatric composite crowns, reconstruction of occlusal wear in posterior composite restorations, establishment of edge length incisal before the aesthetic lengthening of the crown and the development of compound prototypes for milling. In addition, this technique can be used to establish the vertical dimension and to alter the occlusal schemes (anterior guide and posterior deocclusion) before obtaining the final restorations. It is a non-invasive technique that is also used to improve communication between the patient and the restorative team during treatment planning. [1]. The objective of this work is to demonstrate that the fluid resin injection technique is a good procedure that, supported by tools such as mock up, gives us excellent aesthetic and functional results.

Presentation of the case

25-year-old female patient who goes to dental consultation for teeth whitening, when diagnosing the case, the presence of diastema was observed in the upper centrals, as well as anomalies regarding aesthetic smile parameters such as pigmentation, proportions, incisal edge line, among other things. Diagnostic waxing, mockup and photographs were performed to evaluate the result. The treatment plan consisted of 6 resin veneers made with the fluid resin injection technique through a transparent silicone matrix (Flow injection technique).

Clinical procedure

Figure 1 DSD
Source: Self Made

Figure 2 Diagnostic Waxing
Source: Self Made

Figure 3
Source: Self Made

Figure 4
Source: Self Made

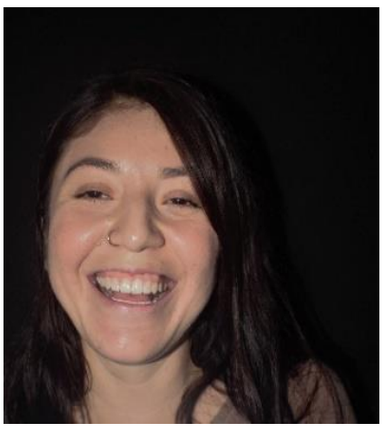

Figure 5 Mockup analysis
Source: Self Made

Figure 6 Procedure
Source: Self Made

ISSN-On line: 2410-4191

Figure 7 Polishing system
Source: Self Made

Figure 8 Before and After
Source: Self Made

Figure 9 Before and After
Source: Self Made

Study models, photographs, prior anamnesis and clinical history filling were made, diagnostic waxing was obtained with additive technique (Renfert modeling wax) for which the obtained DSD (Img. 1 and 2) was taken as a reference, it was used PK Thomas hand instrument.

The result was subsequently proposed to the patient by means of a mock up (Img. 3 polymethyl siloxane and acrylic resin) with which the situation at the mouth of what was obtained in the waxing was analyzed (Img. 4 and 5)

We proceed to perform the fluid resin injection technique for which a transparent polyvinyl siloxane silicone matrix (Memosil 2) was obtained from the diagnostic waxing, which was made holes with round milling cutter of carbide number 8 and micromotor in the area of incisal edges of the teeth 13 to 23, the surpluses were cleaned with alcohol, each tooth was isolated from its adjacent ones with Teflon tape, the preparation of the dental substrate was carried out: total etching (ultra etch phosphoric acid 35%), washing, adhesive placement (Peak universal bond) and light-curing for 20 seconds with bluephase lamp (ivoclar vivadent).

Once the process was finished, the transparent silicone matrix was brought to the mouth and fluid resin (tetric N Flow color bleach) was injected through the previously made hole, light-cured, and after removal of the matrix, excess surpluses were removed. resin with a scalpel blade (no. 12). The same procedure was applied for each tooth (Img 6). To finish the polishing of the veneers was carried out by means of rubber cups of thick, medium and fine grain respectively (jiffy) and was finished with horse hair and cotton tassel, all this with a low speed engine at 10,000 rpm. (Img. 7).

Results

The prognosis of the case is considered favorable, taking into account that the resin treatment is not definitive, however, the functional and aesthetic results were obtained properly (Img. 8 and 9).

Conclusions

Mock up is a necessary tool for obtaining predictable treatments, it allows us to preview the treatment plan and its aesthetic and functional analysis5. The fluid resin injection technique is a minimally invasive technique through which we obtain aesthetic and functional treatments, its greatest disadvantage is its durability since it is not considered a definitive treatment1.

ISSN-On line: 2410-4191

It is possible to perform aesthetic and functional treatments with cheaper materials than porcelain, such is the case of composite resin.

References

[1]Terry D, Powers J. (2015) Using injectable resin composite: part one, INTERNATIONAL DENTISTRY-AFRICAN EDITION, VOL. 5 NO. 1, pgs. 52-62.

[2]Alothman Y, Saleh M. (2018) The succes of Dental Veneers According To Preparation Design and Material Type, Journal of Medical Science.

[3]Orr C. (2016) 'State of the art' in aesthetic dentistry, British Dental Journal, Volume 221 No. 8.

[4]Cohelo F, Silveira D, Peres Michele, y col. (2015). Direct anterior composite veneres in vital and not vital teeth, Journal of Dentistry, Elsevier, Brazil.

[5]Yassine H. (2016) El Mockup, Dental Tribune Hispanic and Latin America.

[6]Lamas C, Angulo de la Vega G. Reconstrucción del Sector Anterior con resinas compuestas, Odontol. G. (2016). La supervivencia de las restauraciones directas de composite en el manejo del desgaste dental severo que incluye desgaste y erosión: un estudio prospectivo de 8 años. Jornal of Dentistry, Elsevier.

[7]Orozco J, Berrocal J, Diaz A. (2015). Composite veneers as an alternative to ceramic veneers in the treatment of dental anomalies. Case report. Revista clínica de periodoncia, implantología y rehabilitación oral.

[8]Pontes P, Goulart da Costa R, Clagaro M, y col. (2018) Diseño de sonrisa digital y técnica de maqueta para la planificación del tratamiento estético con carillas de porcelana laminada, Journal of conservative dentistry.

[9]Terry D, Powers J. Using injectable resin composite, part two. http://www.moderndentistrymedia.com/jan_feb 2015/terr_part-two.pdf.

[10]Eng E, Jorge Ulloa. (2019) Dental Veneers with injectable composite resine technique. Case Report. Revista Científica Universitaria de las Ciencias d

ISSN-On line: 2410-4191

Article **ECORFAN-Journal Bolivia**
December 2019 Vol.6 No.11 35-41

Sequence of treatment of a labial hemangioma

Secuencia de tratamiento de un hemangioma labial

ACUÑA-GONZALEZ, Gladys Remigia†, MAYA-GARCÍA, Ixchel, ROSADO-VILA, Graciella and ZAPATA-MAY, Rafael

Universidad Autonoma de Campeche, Faculty of Odontology and Faculty of Nursing, San Francisco de Campeche, México

ID 1st Author: *Gladys Remigia, Gonzalez-Acuña* / **ORC ID**: 0000-0002-7739-2001

ID 2nd Coauthor: *Ixchel, Maya-García* / **ORC ID**: 0000-0002-4951-3216

ID 2nd Coauthor: *Graciella, Rosado-Vila* / **ORC ID** 0000-0002-8688

ID 3rd Coauthor: *Rafael, Zapata-May* / **ORCID** 0000-0002-3750

DOI: 10.35429/EJB.2019.11.6.35.41 Received: September 09, 2019; Accepted: December 30, 2019

Abstract

This paper presents the case of a woman of forty- four years old, wich go for volumen increase, violet color more tan ten years of evolution in lower lip, greather growth in tle last year. This papaer shows the treatment sequence by placling of cooper needles and subsecuent satisfactory resección restricting risk of bleeding to mínimum.

Labial hemangioma, Vascular injures, Cooper needles, Wires cooper

Resumen

Se presenta el caso de un paciente del sexo femenino que se presenta por aumento de volumen violáceo de más de 10 años de evolución en labio inferior con incremento en el tamaño de la lesión en el último año. Se muestra la secuencia clínica de tratamiento mediante la colocación preqirurgica de agujas de cobre y posterior resección satisfactoria de la lesión restringiendo riesgo de sangrado al mínimo.

Hemangioma labial, Malformaciones venosas, Agujas de cobre

Citation: ACUÑA-GONZALEZ, Gladys Remigia, MAYA-GARCÍA, Ixchel, ROSADO-VILA, Graciella and ZAPATA-MAY, Rafael. Sequence of treatment of a labial hemangioma. ECORFAN Journal-Bolivia. 2019. 6-11: 35-41

† Researcher contributing as first author.

Introduction

Vascular lesions represent a group of relatively frequent lesions in dental practice and in the maxillofacial region. In 1982, Mulliken and Glowacki classify them into two large groups: hemangiomas and vascular malformations, this classification was modified in 1996 by the International Society for the Study of Vascular Abnormalities (ISSVA) proposing a new internationally accepted classification.

Classification of vascular anomalies ISSVA 1996

Vascular tumors	Vascular malformations
Hemangioma	Capillaries
Kaposiform hemangioendothelioma	Venous
Angioma in plume	Lymphatic
Hemangiopericytoma	Arteriovenous
Pyogenic Granuloma	Combined
Spindle-cell hemangioendothelioma	

In children, spontaneous involution has been described, involving minimal or no sequelae.

Etiology

Vascular lesions of the skin represent a very frequent anomaly; They can range from a pink macula to tumors that can condition disabling malformations. Its etiology is unknown, genetic factors and / or disorders of vasculogenetic activity, and angiogenetic are suspected either during pregnancy, the first months of life or during adulthood.

Vasculogenesis includes the processes that precede the formation of blood vessels from endothelial cells, while the term angiogenesis implies the development of new blood vessels from existing ones.

Angiogenic factors such as vascular endothelial growth factor (VEGF) and fibroblast growth factor (BFGF) are involved in the hemangioma growth phase, and high levels of them can be observed in affected patients (1).

Clinical manifestations

Its cynical manifestation is usually diverse, and diversity is related to its depth, location and degree of evolution.

According to the anatomical structures involved, they can be superficial, deep or subcutaneous and mixed when they involve both superficial and deep tissues.

Superficial hemangiomas can be flat or raised with regular or not bright red borders. (Formerly called capillaries, in strawberry or strawberry).

The deep or subcutaneous ones are usually delimited by transparent with bluish or violet color and previously they were known as “cavernous” attributed to blood vessels of greater caliber than the superficial ones.

The mixed ones have combined characteristics of the previous two and can be single or multiple and must carry out complementary diagnostic studies to rule out the presence of multiple organic lesions in special cases.

The most frequent topographies are: head and neck 60%, trunk 25% and limbs 15%. According to Fernanda Salvo and Cols 65% of them are superficial, 15% deep and 20% mixed.

Vascular malformations

Bleeding is a common feature when it comes to removing these lesions surgically so their diagnosis, management and location should be extensively studied.

Mulliken and Enjolras distinguish those with high vascular flow (arteriovenous malformations) and those with low vascular flow (capillary, venous and lymphatic malformations), based on their location, biological, histological and clinical behavior. (1,2)

It is possible to observe combinations of malformations as part of complex syndromes that require combined or special treatments.

The most frequently affected places in the mouth are the lips, tongue and jugular mucosa.

– The size of mouth hemangiomas varies from a few millimeters to extensive lesions that can cause deformities such as macroglossia or macrocheilia.

ISSN-On line: 2410-4191

– About 10 percent of hemangiomas are congenital. Some tend to disappear spontaneously and are called immature hemangiomas.

– A characteristic sign of the lesion is that, when pressed with a finger, the red color disappears and reappears when pressure is stopped. (3)

Study approach

In those cases of large lesions or in the case of suspected multiple lesions, it will be convenient to supplement with special imaging studies such as ultrasound, computed tomography (CT) or Magnetic Resonance Imaging (MRI) if necessary.

Treatment

There are various techniques all aimed at the disappearance of the lesion, which when it appears congenitally or during the first months of life if it is not large usually involves.

Some treatment alternatives described are:

a. Systemic steroids (Prednisone) in doses of 2 to 5 mg / Kg / day until the desired regression is obtained.
b. Intralesional corticosteroids such as triamsinolone alone or associated with dexamethasone sclerotherapy offer the risk of necrosis, allergic reactions and scars.
c. Sclerotherapy based on solutions such as 3% polidocanol in children and adolescents has been reported effectively.
d. Interferon - alpha for antiproliferative and antiangiogenic purposes in the form of subcutaneous or intramuscular injections with side effects including fever, fatigue, vertigo, leukopenia, thrombocytopenia, liver damage, thyroid function disorders and neurotoxicity.
e. Use of laser especially effective in superficial and small lesions, since in large lesions occasionally ulceration and secondary infection may occur.
f. Needles or copper wires. Based on the observations of the peasants who notice that a minor injury when punctured or ulcer reduces in size, Wang in 1993 in China, recommended puncturing venous malformations with copper needles and applying light electric shocks on them. We modified the method: we implanted simple copper wires using a long straight needle and under local anesthesia on an outpatient basis, creating a wire grid in the lesion. Weekly they are extracted. The irritation we produce stimulates intravascular coagulation and when the clots are reabsorbed, the malformation disappears or so Less reduces considerably in size. If necessary, then dry the excess skin under local anesthesia

Also on an outpatient basis Intralesional copper needles. Coiffman (2007) modified the technique by inserting copper needles as a grid omitting electric shocks.

g. In 2008, the use of propanolol in hemangiomas was published, when used for the treatment of cardiac complications derived from prolonged use of corticosteroids in patients with hemangiomas The use of propanolol has been an alternative treatment that has shown positive results especially in hemangiomas in children (4,5)
h. Surgery has proven useful for resection of residual lesions. The use of compressive bandages for the treatment of minor limb injuries has been reported in some cases. Cryosurgery offers the risk of scar injuries.

Radiation therapy is not an alternative in the treatment of hemangiomas since they are benign lesions that do not respond to this treatment. (8,9,10)

Presentation of the case

This is a female patient who comes to the consultation with a history of volume increase in the lower lip of approximately 10 years of evolution, initially asymptomatic, however, during the last year, progressive growth of the lesion accompanied by intermittent pain. Alternate events of greater growth that prevent food.

ISSN-On line: 2410-4191

There is a well-defined lesion larger than 2cm in diameter, well-defined edges which shows ischemia at the digits pressure and volume recovery when removing local pressure. It was decided to initiate a treatment protocol with the placement of copper needles in order to reduce the size of the lesion, taking a weekly check after their placement.

Occupational income manifestations

Figure 1

Increase in the volume of deforming violet color in the central area of the lip at the time of initial assessment.

The initial placement of low copper needles is established as a treatment plan

Local anesthesia in order to reduce the size of the lesion after resection.

Copper caliber segments are prepared and sterilized and placed on an outpatient basis under local anesthesia.

Sequence in the placement of copper needles

Figure 2

Local anesthesia prior placement of copper needles

Figure 3

Needle placement is initiated, the change in the color of the lesion upon introduction to the needle is evident

Figure 4

Needle placement is concluded without adverse events

The copper needles are kept for one week giving only as a complementary treatment amoxicillin 500mg orally every 8 hours and lysine clonixinate 250mg tablets every 6 hours for 3 to 5 days depending on pain, citing a week after withdrawal.

Needle control and removal images

Figure 5

ACUÑA-GONZALEZ, Gladys Remigia, MAYA-GARCÍA, Ixchel, ROSADO-VILA, Graciella and ZAPATA-MAY, Rafael. Sequence of treatment of a labial hemangioma. ECORFAN Journal-Bolivia. 2019

ISSN-On line: 2410-4191

Figure 6

Appearance of the lesion at 48 hours and one week after coloring to monitor evolution and their removal

One week after the initial treatment, a control appointment for needle removal is granted AND Close monitoring is continued to regulate conduct to be followed.

Figure 7

Characteristics of the lip three weeks after needle placement and removal

After the placement of needles, it was possible to observe the decrease in the diameter and depth of the hemangioma by more than fifty percent, thus reducing the risk of trans-surgical active bleeding and once the healing of the placement sites is guaranteed, the removal of the remaining lesion.

Resection of residual injury

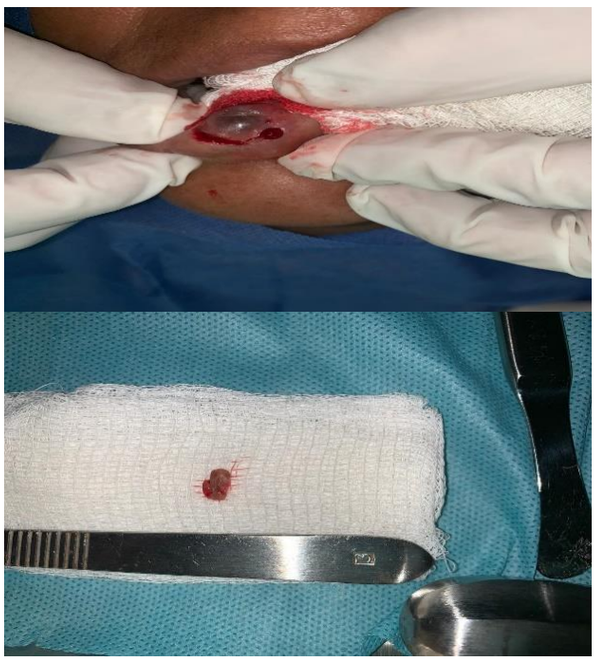

Figure 8

Final resection of the lesion with minimal bleeding

Post-Surgical Follow-Up

Figure 9

ISSN-On line: 2410-4191

Follow-up 10 days after the removal of a residual lesion

Figure 10

Clinical appearance of lip at 2 weeks postoperatively

Conclusion

Hemangiomas are vascular lesions that offer aesthetic and functional alterations to the patient but above all they offer a risk of significant bleeding during their resection, although there is successful evidence of their removal by laser surgery, it remains an alternative treatment the use of copper needles in order to reduce their size and vascular flow, provided that the patient's systemic conditions allow it.

References

[1] 2 María Rosa Cordisco.Marzo- Junio(2003)Medicina Infantil Vol. X. No. 1 y 2. http://www.medicinainfantil.org.ar

[2] Tratamiento de las malformaciones venosas con alambre de cobre. Coiffman, F. *..Cirugía Plástica Ibero-Latinoamericana versión On-line ISSN 1989-2055versión impresa ISSN 0376-7892 Cir. plást. iberolatinoam. vol.37 no.2 Madrid abr./jun. 2011. http://dx.doi.org/10.4321/S0376-78922011000200008 SciELO - Scientific Electronic Library Online

[3] Hemangioma cavernoso a propósito de dos casos en atención primaria.
Dr. Aitziber Ugalde Olano. Adjunto Anatomía Patológica. Hospital de Mendaro, Guipúzcoa
Gaceta Dental. Octubre 2011. https://gacetadental.com/2011/10/hemangioma-cavernoso-a-propsito-de-dos-casos-en-atencin-primaria-25274/

[4] Propanolol en el tratamiento de los hemangiomas: una alternativa terapéutica. Caso clínico. Fernanda Salvo, Nancy De Olivera, Mariela Álvarez, Gustavo Giachett. Arch. Pediatr. Urug. vol.85 no.2 Montevideo June 2014 On-line version ISSN 1688-1249

[5] Tratamiento de las malformaciones venosas con alambres de cobre. Coiffman, F.* Cir.plást. iberolatinoam.-Vol. 37 - Nº 2 Abril - Mayo - Junio 2011 / Pag. 155-160 Cirugía Plástica Ibero – Latinoamericana.

[6] Inserción de agujas de cobre dispuestas en forma deasterisco para el tratamiento de un hemangioma cavernoso en boca. Narváez-Chávez A, Peñaloza-Cuevas R, Rodríguez-Fernández MSC, Lama-González EM.Facultad de Odontología, Universidad Autónoma de Yucatán. Revista Odontológica Latinomaericana (2014) Vol. 6 | Núm. 2 | pp 41-44.

[7] Escleroterapia en el tratamiento de hemangiomas de los tejidos blandos de la cavidad bucal en estomatología pediátrica. Cecilia Jiménez Palacios. Acta odontológica Venezolana ISNN: 0001-6335. Vol. 97 No. 4 año 2009.

[8] Hemangioma del labio superior tratado con éxito con propanolol. Autores: Madrigal Díez Ca, Mazas Raba MRb, Fernández Jiménez MIc, De Diego García EMd, Ballestero Diego R. Pediatra. CS Bezana. Rev Pediatr Aten Primaria. 2011;13:233-40.

[9] Cirugía Transoral en hemangiomas de laringe e hipofaringe en adultos. Eduardo Figueroa, Fabricio Ianardi, Andrés Vega Morejón y Carlos Santiago Rugger Rev. Hosp. Ital. B.Aires 2018; 38(3): 115-118

ISSN-On line: 2410-4191

[10] Hemangioma capilar versus granuloma telangiectásico en cavidad bucal; una ardua labor diagnostica. Martha Leonor Rebolledo-Cobos y Manuel Vicente Escalante-Fontalvo. Revista Duazary ISSN: 1794-5992 Vol. 12 No. 2 187 - 191 Julio - Diciembre de 2015.

ISSN-On line: 2410-4191

[Title in Times New Roman and Bold No. 14 in English and Spanish]

Surname (IN UPPERCASE), Name 1st Author†*, Surname (IN UPPERCASE), Name 1st Coauthor, Surname (IN UPPERCASE), Name 2nd Coauthor and Surname (IN UPPERCASE), Name 3rd Coauthor

Institutional Affiliation of Author including Dependency (No.10 Times New Roman and Italic)

International Identification of Science - Technology and Innovation

ID 1st author: (ORC ID - Researcher ID Thomson, arXiv Author ID - PubMed Author ID - Open ID) and CVU 1st author: (Scholar-PNPC or SNI-CONACYT) (No.10 Times New Roman)

ID 1st coauthor: (ORC ID - Researcher ID Thomson, arXiv Author ID - PubMed Author ID - Open ID) and CVU 1st coauthor: (Scholar or SNI) (No.10 Times New Roman)

ID 2nd coauthor: (ORC ID - Researcher ID Thomson, arXiv Author ID - PubMed Author ID - Open ID) and CVU 2nd coauthor: (Scholar or SNI) (No.10 Times New Roman)

ID 3rd coauthor: (ORC ID - Researcher ID Thomson, arXiv Author ID - PubMed Author ID - Open ID) and CVU 3rd coauthor: (Scholar or SNI) (No.10 Times New Roman)

(Report Submission Date: Month, Day, and Year); Accepted (Insert date of Acceptance: Use Only ECORFAN)

Abstract (In English, 150-200 words)

Objectives
Methodology
Contribution

Abstract (In Spanish, 150-200 words)

Objectives
Methodology
Contribution

Keywords (In English)

Indicate 3 keywords in Times New Roman and Bold No. 10

Keywords (In Spanish)

Indicate 3 keywords in Times New Roman and Bold No. 10

Citation: Surname (IN UPPERCASE), Name 1st Author†*, Surname (IN UPPERCASE), Name 1st Coauthor, Surname (IN UPPERCASE), Name 2nd Coauthor and Surname (IN UPPERCASE), Name 3rd Coauthor. Paper Title. ECORFAN Journal. Year 1-1: 1-11 [Times New Roman No.10]

---

* Correspondence to Author (example@example.org)
† Researcher contributing as first author.

Introduction

Text in Times New Roman No.12, single space.

General explanation of the subject and explain why it is important.

What is your added value with respect to other techniques?

Clearly focus each of its features

Clearly explain the problem to be solved and the central hypothesis.

Explanation of sections Article.

Development of headings and subheadings of the article with subsequent numbers

[Title No.12 in Times New Roman, single spaced and bold]

Products in development No.12 Times New Roman, single spaced.

Including graphs, figures and tables-Editable

In the article content any graphic, table and figure should be editable formats that can change size, type and number of letter, for the purposes of edition, these must be high quality, not pixelated and should be noticeable even reducing image scale.

[Indicating the title at the bottom with No.10 and Times New Roman Bold]

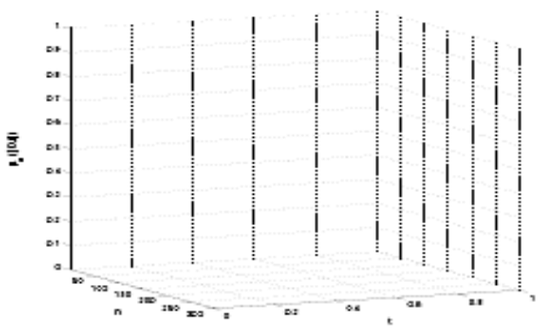

Graphic 1 Title and *Source (in italics)*

Should not be images-everything must be editable.

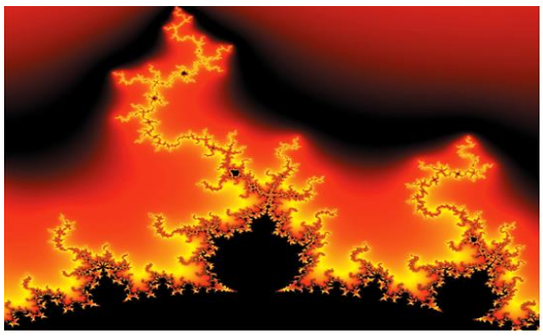

Figure 1 Title and *Source (in italics)*

Should not be images-everything must be editable.

Table 1 Title and *Source (in italics)*

Should not be images-everything must be editable.

Each article shall present separately in **3 folders**: a) Figures, b) Charts and c) Tables in .JPG format, indicating the number and sequential Bold Title.

For the use of equations, noted as follows:

$$Y_{ij} = \alpha + \sum_{h=1}^{r} \beta_h X_{hij} + u_j + e_{ij} \qquad (1)$$

Must be editable and number aligned on the right side.

Methodology

Develop give the meaning of the variables in linear writing and important is the comparison of the used criteria.

Results

The results shall be by section of the article.

Annexes

Tables and adequate sources thanks to indicate if were funded by any institution, University or company.

Conclusions

Explain clearly the results and possibilities of improvement.

ISSN: 2410-4191

References

Use APA system. Should not be numbered, nor with bullets, however if necessary numbering will be because reference or mention is made somewhere in the Article.

Use Roman Alphabet, all references you have used must be in the Roman Alphabet, even if you have quoted an Article, book in any of the official languages of the United Nations (English, French, German, Chinese, Russian, Portuguese, Italian, Spanish, Arabic), you must write the reference in Roman script and not in any of the official languages.

Technical Specifications

Each article must submit your dates into a Word document (.docx):

Journal Name
Article title
Abstract
Keywords
Article sections, for example:

1. Introduction
2. Description of the method
3. Analysis from the regression demand curve
4. Results
5. Thanks
6. Conclusions
7. References

Author Name (s)
Email Correspondence to Author
References

Intellectual Property Requirements for editing:

-Authentic Signature in Color of Originality Format Author and Coauthors

-Authentic Signature in Color of the Acceptance Format of Author and Coauthors

ISSN: 2410-4191

Reservation to Editorial Policy

ECORFAN-Journal Bolivia reserves the right to make editorial changes required to adapt the Articles to the Editorial Policy of the Journal. Once the Article is accepted in its final version, the Journal will send the author the proofs for review. ECORFAN® will only accept the correction of errata and errors or omissions arising from the editing process of the Journal, reserving in full the copyrights and content dissemination. No deletions, substitutions or additions that alter the formation of the Article will be accepted.

Code of Ethics - Good Practices and Declaration of Solution to Editorial Conflicts

Declaration of Originality and unpublished character of the Article, of Authors, on the obtaining of data and interpretation of results, Acknowledgments, Conflict of interests, Assignment of rights and Distribution.

The ECORFAN-Mexico, S.C Management claims to Authors of Articles that its content must be original, unpublished and of Scientific, Technological and Innovation content to be submitted for evaluation.

The Authors signing the Article must be the same that have contributed to its conception, realization and development, as well as obtaining the data, interpreting the results, drafting and reviewing it. The Corresponding Author of the proposed Article will request the form that follows.

Article title:

- The sending of an Article to ECORFAN -Journal Bolivia emanates the commitment of the author not to submit it simultaneously to the consideration of other series publications for it must complement the Format of Originality for its Article, unless it is rejected by the Arbitration Committee, it may be withdrawn.

- None of the data presented in this article has been plagiarized or invented. The original data are clearly distinguished from those already published. And it is known of the test in PLAGSCAN if a level of plagiarism is detected Positive will not proceed to arbitrate.

- References are cited on which the information contained in the Article is based, as well as theories and data from other previously published Articles.

- The authors sign the Format of Authorization for their Article to be disseminated by means that ECORFAN-Mexico, S.C. In its Holding Bolivia considers pertinent for disclosure and diffusion of its Article its Rights of Work.

- Consent has been obtained from those who have contributed unpublished data obtained through verbal or written communication, and such communication and Authorship are adequately identified.

- The Author and Co-Authors who sign this work have participated in its planning, design and execution, as well as in the interpretation of the results. They also critically reviewed the paper, approved its final version and agreed with its publication.

- No signature responsible for the work has been omitted and the criteria of Scientific Authorization are satisfied.

- The results of this Article have been interpreted objectively. Any results contrary to the point of view of those who sign are exposed and discussed in the Article.

Copyright and Access

The publication of this Article supposes the transfer of the copyright to ECORFAN-Mexico, SC in its Holding Bolivia for its ECORFAN -Journal Bolivia, which reserves the right to distribute on the Web the published version of the Article and the making available of the Article in This format supposes for its Authors the fulfilment of what is established in the Law of Science and Technology of the United Mexican States, regarding the obligation to allow access to the results of Scientific Research.

Article Title:

Name and Surnames of the Contact Author and the Coauthors	Signature
1.	
2.	
3.	
4.	

Principles of Ethics and Declaration of Solution to Editorial Conflicts

Editor Responsibilities

The Publisher undertakes to guarantee the confidentiality of the evaluation process, it may not disclose to the Arbitrators the identity of the Authors, nor may it reveal the identity of the Arbitrators at any time.

The Editor assumes the responsibility to properly inform the Author of the stage of the editorial process in which the text is sent, as well as the resolutions of Double-Blind Review.

The Editor should evaluate manuscripts and their intellectual content without distinction of race, gender, sexual orientation, religious beliefs, ethnicity, nationality, or the political philosophy of the Authors.

The Editor and his editing team of ECORFAN® Holdings will not disclose any information about Articles submitted to anyone other than the corresponding Author.

The Editor should make fair and impartial decisions and ensure a fair Double-Blind Review.

Responsibilities of the Editorial Board

The description of the peer review processes is made known by the Editorial Board in order that the Authors know what the evaluation criteria are and will always be willing to justify any controversy in the evaluation process. In case of Plagiarism Detection to the Article the Committee notifies the Authors for Violation to the Right of Scientific, Technological and Innovation Authorization.

Responsibilities of the Arbitration Committee

The Arbitrators undertake to notify about any unethical conduct by the Authors and to indicate all the information that may be reason to reject the publication of the Articles. In addition, they must undertake to keep confidential information related to the Articles they evaluate.

Any manuscript received for your arbitration must be treated as confidential, should not be displayed or discussed with other experts, except with the permission of the Editor.

The Arbitrators must be conducted objectively, any personal criticism of the Author is inappropriate.

The Arbitrators must express their points of view with clarity and with valid arguments that contribute to the Scientific, Technological and Innovation of the Author.

The Arbitrators should not evaluate manuscripts in which they have conflicts of interest and have been notified to the Editor before submitting the Article for Double-Blind Review.

Responsibilities of the Authors

Authors must guarantee that their articles are the product of their original work and that the data has been obtained ethically.

Authors must ensure that they have not been previously published or that they are not considered in another serial publication.

Authors must strictly follow the rules for the publication of Defined Articles by the Editorial Board.

The authors have requested that the text in all its forms be an unethical editorial behavior and is unacceptable, consequently, any manuscript that incurs in plagiarism is eliminated and not considered for publication.

Authors should cite publications that have been influential in the nature of the Article submitted to arbitration.

Information services

Indexation - Bases and Repositories

LATINDEX (Scientific Journals of Latin America, Spain and Portugal)
RESEARCH GATE (Germany)
GOOGLE SCHOLAR (Citation indices-Google)
REDIB (Ibero-American Network of Innovation and Scientific Knowledge- CSIC)
MENDELEY (Bibliographic References Manager)

Publishing Services:

Citation and Index Identification H.
Management of Originality Format and Authorization.
Testing Article with PLAGSCAN.
Article Evaluation.
Certificate of Double-Blind Review.
Article Edition.
Web layout.
Indexing and Repository
ArticleTranslation.
Article Publication.
Certificate of Article.
Service Billing.

Editorial Policy and Management

21 Santa Lucía, CP-5220. Libertadores -Sucre–Bolivia. Phones: +52 1 55 6159 2296, +52 1 55 1260 0355, +52 1 55 6034 9181; Email: contact@ecorfan.org www.ecorfan.org

ECORFAN Journal-Bolivia

2410-4191
ISSN 2410-4191

www.ecorfan.org